Acta Geochim (2020) 39(5):616–641
https://doi.org/10.1007/s11631-020-00425-3

ORIGINAL ARTICLE

Geochemical constraints on the origin of Early Cretaceous alkaline intrusions and its tectonic implication, Sulu Orogenic Belt, Eastern North China Craton

Shen Liu[1] · Caixia Feng[1] · Yan Fan[1] · Kairui Tai[1] · Tianjing Gao[1] · Ian M. Coulson[2]

Received: 18 May 2020 / Revised: 15 July 2020 / Accepted: 29 July 2020 / Published online: 13 August 2020

Abstract Post-orogenic alkaline intrusions from the Sulu Orogenic Belt of eastern North China Craton consist of A-type granites. In this study, we report U–Pb zircon ages, geochemical data, Sr–Nd–Pb, and zircon Hf isotopic data for these rocks. The LA-ICP-MS U–Pb zircon analyses yield consistent ages ranging from 127.1 ± 2.4 to 119.5 ± 4.8 Ma for four samples. The alkaline rocks are characterized by high total alkalis (K_2O + Na_2O = 8.32–10.11 wt%), light rare-earth element enrichment, and heavy rare-earth element depletion, with a wide range $(La/Yb)_N$ values (20–48), moderate negative Eu anomalies (Eu/Eu* = 0.50–0.74), enrichment in large-ion lithophile elements (LILEs, i.e., Rb, Th, U and Pb), and depletion in Ba, Sr and high field strength elements (HFSEs, i.e., Nb, Ta, and Ti), high $(^{87}Sr/^{86}Sr)_i$ ranging from 0.708 to 0.7089, low ε_{Nd} (t) values from −19.4 to −16.8, $(^{206}Pb/^{204}Pb)_i$ = 16.751 – 16.935, $(^{207}Pb/^{204}Pb)_i$ = 15.381−15.535, $(^{208}Pb/^{204}Pb)_i$ = 37.472–37.838, negative ε_{Hf} (t) values between −21.3 and −25.7 for the magmatic zircons, and larger T_{DM2} model ages from 2.5 to 2.8 Ga. These results suggest that the rocks were derived from a common enriched lithospheric mantle source that was metasomatized by foundered lower crustal eclogitic materials before magma generation. Furthermore, the geochemical and isotopic feature implies that the primary magma of these rocks originated through partial melting of ancient lithospheric mantle that was variably hybridized by melts derived from lower crust eclogite. These rocks in this study may have been generated by subsequent fractionation of potassium feldspar, plagioclase, ilmenite, and/or rutile. However, negligible crustal contamination occurred during the diagenesis process.

Keywords Post-orogenic magmatism · Alkaline rocks · Contamination · Sulu Orogenic Belt · North China Craton

1 Introduction

As a typical Archaean craton, the North China Craton (NCC) exhibits distinct characteristics from other cratons (Menzies et al. 2007; Griffin et al. 1998; Menzies and Xu 1998; Xu et al. 1998a, b; Fan et al. 2000; Zheng et al. 2001, 2006; Gao et al. 2002, 2004; Zhang et al. 2002, 2003; Wu et al. 1998, 2003, 2005a, b, 2006; Chen et al. 2004; Wilde et al. 2004; Zhai et al. 2007). For example, strong lithospheric destruction has occurred since the Mesozoic. Nevertheless, there are still many controversial issues concerning the destruction of the NCC, such as the destruction time, space, mechanism, and control factors (Wu et al. 2006; Yang et al. 2006; Menzies et al. 2007; Zhai et al. 2007; Zhang et al. 2007; Zheng et al. 2007; Wu et al. 1998; Liu et al. 2008a, b, 2009; 2013c). The main reasons for the above disagreement are the lack of understanding of Mesozoic lithospheric mantle properties and deep processes beneath the NCC (Wu et al. 1998). In recent years, it is generally accepted that the NCC was in an extensional tectonic background during Mesozoic (Wu et al. 1998). Therefore, it is particularly important to study the chronology, elements, and isotope geochemistry of mantle-derived magmatic rocks produced in an extensional setting (e.g., mafic dykes, carbonates and alkaline rocks).

✉ Shen Liu
liushen@nwu.edu.cn

[1] State Key Laboratory of Continental Dynamics, Department of Geology, Northwest University, Xi'an 710069, China

[2] Solid Earth Studies Laboratory, Department of Geology, University of Regina, Regina, SK S4S 0A2, Canada

Mesozoic mafic dykes and carbonates are widely spread in the NCC. More than 200 dykes has been found, and the mafic dykes are mostly distributed along the NE, NW, and EW directions, the length of them is between 10 and 35 km, and the width is more than 8.0 km (Cheng et al. 1998; Zhang and Sun 2002; Liu et al. 2004a, b, 2005a, b, 2006, 2008a, b, 2009, 2010a, b, 2012a, b, 2013a, b, d, 2014, 2015, 2016, 2017a, b, 2018; Yang et al. 2004, 2012, 2013a, b; Tang et al. 2014; Guo et al. 2016; Shao et al. 2003, 2005; Yan et al. 2000, 2007; Qiu 1993; Ying et al. 2004).

In contrast, as one special petrographic type, alkaline rocks belong to the alkaline-peralkaline magmatic rocks. They are characterized by unsaturated silicic acid, high alkali content, obvious feldspar, and alkaline dark minerals, and invisible quartz (Harker 1896; Daly 1914; Wright 1969; Irvine and Baragar 1971). Furthermore, alkaline rocks can be subdivided into ultrabasic rocks (e.g., Kimberlite, carbonite, aegirinite, and cabernet sauvignon), basic rocks (e.g., alkaline gabbro and basalt), medium rocks (e.g., alkaline normal-alkaline coarse-nepheline normal-sounding rock), acidic rocks (e.g., alkaline granite, alkaline rhyolite), and alkaline dykes. In general, alkaline rocks are often late products of the magmatic activity in the mantle source region. The study of alkaline rocks thus has important implications for the development, evolution and dynamic processes of orogenic belts (Wu 1966; Ding 1989; Li 1991; Eby 1992; Qiu 1993; Kogarko et al. 1995; Li et al. 1999; Zhou et al. 1995, 2009; Zheng and Bian 1996; Zhang and Xie 1997; Tan 1997; Xu et al. 1998a, b, 2017; Xie et al. 1999, 2006; Altherr et al. 2000; Mingram et al. 2000; Wang et al. 2000; Han 2000; Yan et al. 2000, 2002, 2007; Zhang 2001; Zhang et al. 2002, 2005, 2015; Wu et al. 2002; Litvinovsky et al. 2002; Chen et al. 2003, 2013; Ren et al. 2004; Yang et al. 2005a; Huang et al. 2005, 2016; Ke et al. 2006; Liu et al. 2006, 2008a, 2013c; Wang et al. 2009, 2010a, b; Yu et al. 2010; Chen and Jiang 2011; Kim et al. 2016). However, alkaline rock has not received due attention for a long time because of of its small distribution area (Yan et al. 2002).

In this study, we report new results from LA-ICP-MS zircon U–Pb, major and trace element geochemistry, Sr–Nd–Pb isotopic studies, and zircon Hf data for four

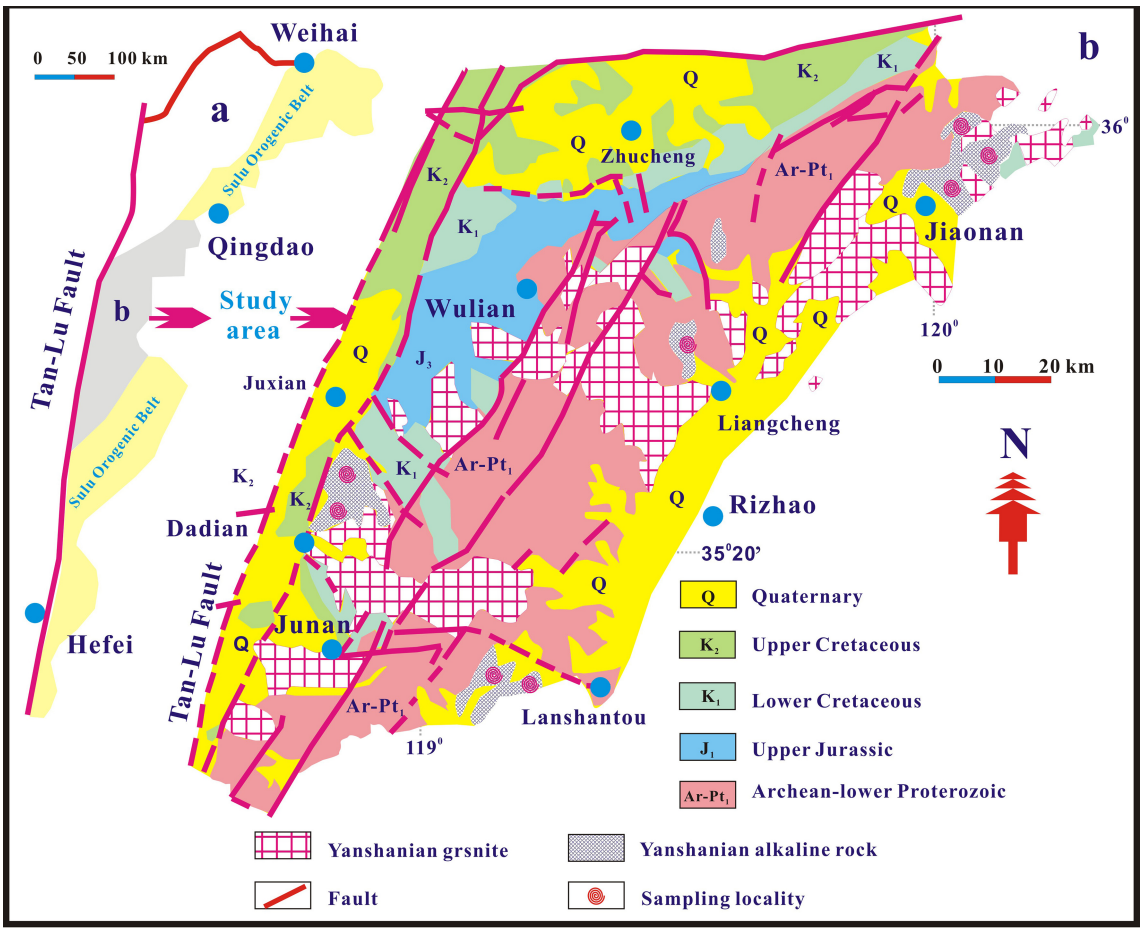

Fig. 1 **a** Simplified tectonic map of the Sulu Orogenic Belt, eastern NCC (Guo et al. 2004). **b** The geologic map of study areas and the distributions of the alkaline intrusions

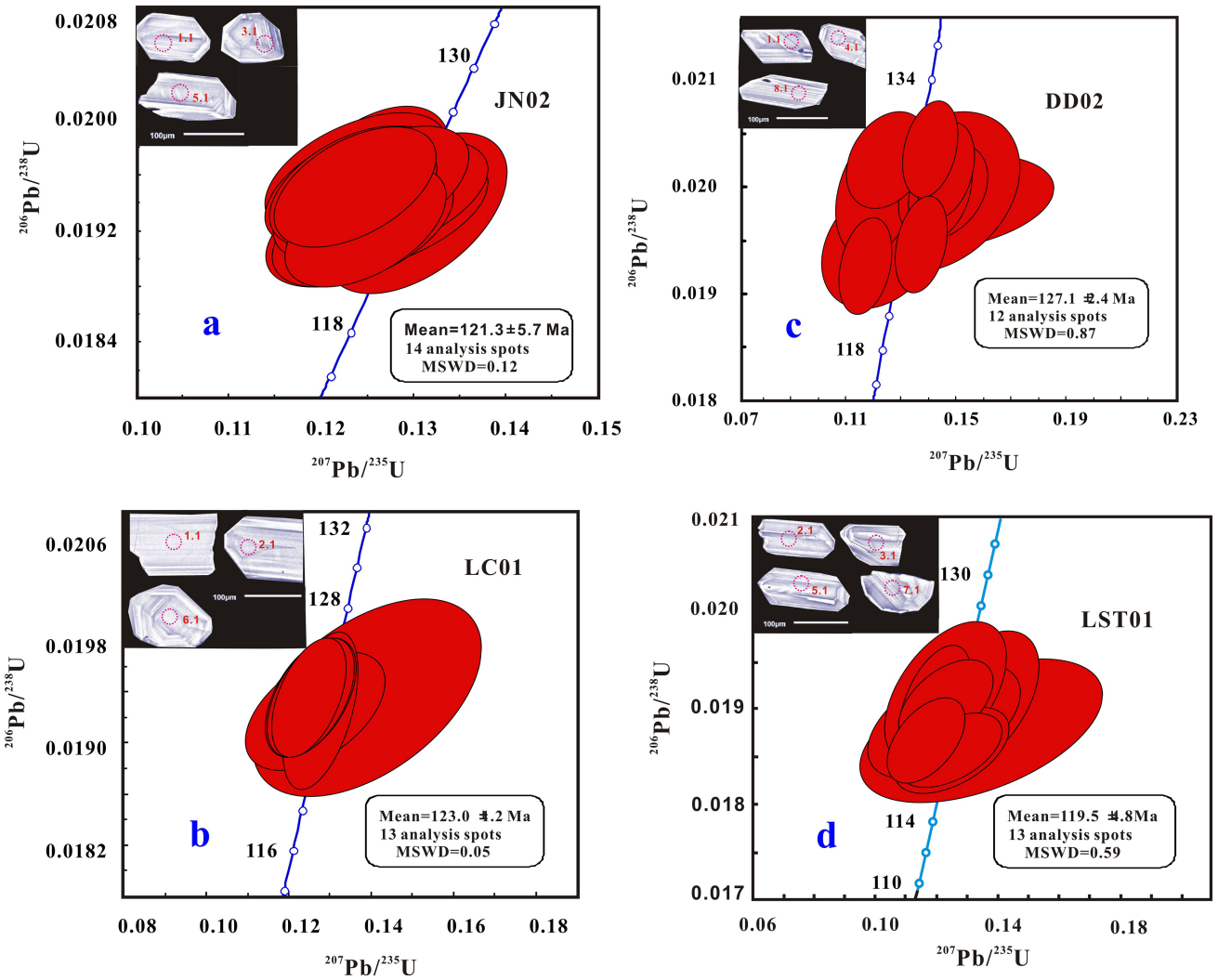

Fig. 2 Representative CL images of zircon grains and zircon LA-ICP-MS zircon U–Pb concordia diagrams for representative A-type granites (JN02, DD02, and LST01) and (LC01) from the Sulu Orogenic Belt, eastern NCC

representative felsic plutons from central Sulu Orogenic Belt. These allow us to: (1) document the reliable age and geochemical characteristics of these rocks; (2) investigate their magma source(s) and origin; and (3) define the tectonic implication during the Early Cretaceous in the study areas.

2 Geological setting and petrography

As the world's largest high-pressure (HP)-ultra-high pressure (UHP) Orogenic rock area, the Sulu Orogenic Belt is located in the eastern part of the NCC. Currently, it has been accepted as the eastern part of Qinling-Dabie collisional Orogenic Belt between the north China and Yangtze Blocks in the Triassic (e.g., Yin and Ni 1993; Ye et al. 1996a, b, 2000; Jahn et al. 1996; Zheng et al. 2002), generally, which can be divided into Orogenic parts, i.e., an HP blueschist unit to the south and a UHP Orogenic granitic gneiss, granulite and subordinate eclogite, schist, amphibolite, marble, and quartzite association unit to the north (Zhai et al. 2000; Chen et al. 2003; Guo et al. 2004). The northern belt also includes Mesozoic Laiyang Basin. In addition, the Sulu orogenic belt is the region with the post-collision magmatic activity during the ultrahigh-pressure and high-pressure rock (e.g., Chung et al. 2005; Dilek and Altunkaynak 2007), especially the Mesozoic magmatism (225–110 Ma; Zhao et al. 1997; Zhou and Lu 2000; Fan et al. 2001; Chen et al. 2003; Zhou et al. 2003; Guo et al. 2004, 2005, 2006; Huang et al. 2005; Zhang et al. 2005; Meng et al. 2005; Yang et al. 2005a, b; Hou et al. 2007; Zhang and Zhang 2007; Liu et al. 2008a, b, 2009, 2013c, 2014; Zhao and Zheng 2009; Zhang et al. 2010; Zhang 2010). Geological data indicate that Mesozoic alkaline

Table 1 Zircon LA-ICP-MS U–Pb isotope data for the alkaline rocks from the Sulu Orogenic Belt, eastern NCC

Spot	Th	U	Pb	Th/U	$^{238}U/^{232}Th$	Isotopic ratios						Age (Ma)					
						$^{207}Pb/^{206}Pb$	1σ	$^{207}Pb/^{235}U$	1σ	$^{206}Pb/^{238}U$	1σ	$^{207}Pb/^{206}Pb$	1σ	$^{207}Pb/^{235}U$	1σ	$^{206}Pb/^{238}U$	1σ
LST01																	
1	586	428	15.4	1.37	1.45	0.0485	0.0042	0.12628	0.0106	0.0186	0.0003	128	158	121	9	119	2
2	636	478	14.8	1.34	1.44	0.0556	0.0073	0.1265	0.0118	0.0186	0.0003	431	181	121	11	118	2
3	488	368	11.2	1.33	0.85	0.0485	0.0041	0.1263	0.0105	0.0187	0.0003	129	158	121	9	119	2
4	382	272	8.26	1.40	0.73	0.0461	0.0032	0.1186	0.0081	0.0187	0.0003	124	155	115	7	119	2
5	295	223	6.88	1.32	0.78	0.0461	0.0051	0.1188	0.0128	0.0186	0.0002	352	218	115	12	119	1
6	235	171	5.15	1.37	0.73	0.0461	0.0031	0.1212	0.0075	0.0191	0.0004	523	144	116	7	122	2
7	231	168	5.24	1.38	0.76	0.0461	0.0038	0.1209	0.0101	0.0191	0.0003	564	185	116	9	122	2
8	286	226	6.93	1.27	0.82	0.0475	0.0036	0.1248	0.0098	0.0191	0.0003	71	181	120	9	122	2
9	242	173	5.41	1.40	0.76	0.0482	0.0045	0.1261	0.0115	0.019	0.0003	106	208	121	10	121	2
10	208	174	5.09	1.20	0.86	0.0515	0.0062	0.1241	0.0158	0.0189	0.0004	262	273	128	14	121	2
11	166	94	3.25	1.77	0.58	0.0522	0.0096	0.1359	0.0251	0.0188	0.0005	295	363	129	22	120	3
12	355	228	6.35	1.56	0.56	0.0586	0.0046	0.1346	0.0128	0.0191	0.0005	555	175	119	10	122	3
13	766	565	15.8	1.36	0.74	0.0586	0.0046	0.1246	0.0126	0.0192	0.0005	555	176	119	11	122	3
LC01																	
1	855	635	16.5	1.35	0.88	0.0535	0.0065	0.1283	0.0115	0.0193	0.0004	351	173	123	11	123	2
2	638	475	16.3	1.34	0.83	0.0562	0.0028	0.1246	0.0066	0.0193	0.0003	455	98	119	6	123	2
3	896	675	17.6	1.33	1.16	0.0583	0.0045	0.1304	0.0115	0.0193	0.0004	545	163	124	10	123	2
4	456	345	11.4	1.32	0.78	0.0516	0.0043	0.1255	0.0105	0.0192	0.0003	267	158	120	9	123	3
5	881	665	17.3	1.32	0.76	0.05445	0.0025	0.1242	0.0058	0.0193	0.0003	392	82	119	5	123	2
6	308	218	6.85	1.41	0.68	0.0535	0.0065	0.1283	0.0115	0.0193	0.0004	351	173	123	10	123	2
7	431	276	8.43	1.56	0.66	0.0562	0.0026	0.1246	0.0068	0.0193	0.0003	455	98	119	6	123	2
8	366	261	9.25	1.40	0.93	0.0535	0.0025	0.1268	0.0056	0.0192	0.0004	352	68	121	5	123	3
9	244	161	5.54	1.52	0.78	0.0583	0.0045	0.1303	0.0115	0.0193	0.0004	544	163	124	11	123	2
10	465	342	13.5	1.36	0.92	0.0516	0.0042	0.1256	0.0105	0.0192	0.0003	266	158	120	9	123	3
11	255	185	5.86	1.38	0.76	0.0545	0.0025	0.1242	0.0056	0.0193	0.0003	391	81	119	5	123	2
12	434	323	10.6	1.34	0.83	0.0545	0.0024	0.1243	0.0058	0.0193	0.0003	385	78	119	5	123	2
13	133	102	3.13	1.30	0.78	0.0517	0.0065	0.1375	0.0172	0.0193	0.0005	275	283	132	15	123	3
DD02																	
1	316	225	7.23	1.40	0.72	0.0558	0.0028	0.1508	0.0068	0.0201	0.0003	446	73	144	6	127	2
2	223	176	5.68	1.27	0.83	0.0461	0.0036	0.1265	0.0098	0.0199	0.0004	553	175	121	9	127	2
3	378	232	7.74	1.63	0.63	0.0554	0.0041	0.1501	0.0105	0.0199	0.0003	428	128	143	9	127	2
4	219	176	5.78	1.24	0.82	0.0542	0.0072	0.1485	0.0191	0.0199	0.0005	376	296	142	17	127	3
5	255	208	6.49	1.23	0.86	0.0589	0.0108	0.1525	0.0245	0.0198	0.0003	565	328	145	22	126	2
6	305	221	6.94	1.38	0.75	0.0553	0.0028	0.1491	0.0075	0.0199	0.0003	426	82	143	7	127	2

Table 1 continued

Spot	Th	U	Pb	Th/U	$^{238}U/^{232}Th$	Isotopic ratios						Age (Ma)					
						$^{207}Pb/^{206}Pb$	1σ	$^{207}Pb/^{235}U$	1σ	$^{206}Pb/^{238}U$	1σ	$^{207}Pb/^{206}Pb$	1σ	$^{207}Pb/^{235}U$	1σ	$^{206}Pb/^{238}U$	1σ
7	228	146	5.02	1.56	0.69	0.0521	0.0038	0.1358	0.0092	0.0197	0.0004	292	123	128	8	126	2
8	356	275	8.49	1.29	0.82	0.0542	0.0025	0.1422	0.0062	0.0194	0.0003	381	74	135	5	124	2
9	216	155	4.85	1.39	0.83	0.0479	0.0055	0.1282	0.0142	0.0194	0.0004	95	238	122	13	124	2
10	233	212	7.73	1.10	0.96	0.0461	0.0025	0.1222	0.0063	0.0192	0.0003	385	118	118	6	123	2
11	336	275	8.78	1.22	0.86	0.0532	0.0025	0.1454	0.0065	0.0203	0.0003	335	75	138	6	129	2
12	337	295	9.36	1.14	0.94	0.0469	0.0035	0.1302	0.0096	0.0202	0.0003	45	166	124	9	129	2
JN02																	
1	1462	355	53.5	4.12	4.16	0.0524	0.0028	0.123	0.006	0.0194	0.0003	305	78	118	5	124	2
2	643	236	46.5	2.72	2.15	0.0523	0.0026	0.122	0.006	0.0195	0.0003	302	78	118	5	124	2
3	458	445	412	1.03	1.56	0.0554	0.0026	0.123	0.006	0.0195	0.0003	428	75	118	5	124	2
4	73	60	12.5	1.20	1.65	0.0518	0.0026	0.126	0.006	0.0195	0.0003	278	78	120	5	124	2
5	364	225	27.2	1.62	1.62	0.0462	0.0028	0.1254	0.0072	0.0194	0.0003	5	98	120	6	124	2
6	425	338	21.3	1.26	1.63	0.0519	0.0028	0.124	0.006	0.0195	0.0004	282	65	118	5	124	3
7	238	121	17.3	1.97	1.62	0.0522	0.0024	0.123	0.006	0.0195	0.0003	295	85	118	6	124	2
8	526	135	161	3.90	1.61	0.0525	0.0025	0.129	0.006	0.0193	0.0004	305	75	123	6	123	3
9	173	135	8.9	1.28	1.58	0.0521	0.0025	0.123	0.006	0.0192	0.0003	290	85	118	6	123	2
10	183	106	11.3	1.73	1.63	0.0525	0.0026	0.124	0.006	0.0192	0.0003	306	75	118	5	123	2
11	536	215	18.4	2.49	2.13	0.0523	0.0025	0.123	0.006	0.0192	0.0003	298	86	118	6	123	3
12	575	158	26.4	3.64	2.12	0.0461	0.0026	0.125	0.007	0.0193	0.0003	277	98	120	6	123	2
13	1265	445	116	2.84	2.12	0.0521	0.0025	0.123	0.006	0.0196	0.0003	290	85	118	6	125	2
14	872	316	32.4	2.76	2.12	0.0519	0.0025	0.125	0.006	0.0196	0.0003	281	78	120	5	125	2

Table 2 Major element concentrations (wt %) for the alkaline rocks from the Sulu Orogenic Belt, eastern NCC; LOI = loss on ignition, $Mg^{\#}$ = 100 Mg/(Mg + Fe) in atomic proportions, RV = recommended values, MV = measured values

Sample	SiO_2	TiO_2	Al_2O_3	Fe_2O_3	MnO	MgO	CaO	Na_2O	K_2O	P_2O_5	LOI	Total	$Mg^{\#}$
JN1	61.95	0.68	15.56	5.21	0.11	2.38	3.92	4.43	5.68	0.42	0.03	100.37	47.5
JN2	61.93	0.73	16.03	5.88	0.10	2.75	4.42	3.63	4.69	0.51	0.03	100.70	48.1
JN3	62.48	0.65	15.72	5.26	0.10	2.51	3.88	4.06	5.48	0.43	0.04	100.61	48.6
JN4	62.51	0.71	15.72	5.41	0.11	2.42	4.02	3.88	5.16	0.44	0.02	100.40	47.0
JN5	62.53	0.65	15.71	5.25	0.10	2.51	3.87	4.09	5.51	0.43	0.03	100.68	48.6
JN6	61.92	0.73	16.02	5.88	0.11	2.75	4.39	3.64	4.68	0.49	0.03	100.64	48.1
JN7	61.86	0.74	16.12	5.76	0.10	2.72	4.31	3.78	4.83	0.50	0.03	100.75	48.3
JN8	62.05	0.66	15.61	5.18	0.11	2.36	3.88	4.42	5.65	0.42	0.03	100.37	47.4
LC1	73.41	0.18	14.28	1.58	0.06	0.36	1.08	3.84	5.71	0.05	0.12	100.67	31.1
LC3	73.32	0.22	13.82	1.66	0.06	0.35	1.26	3.83	5.05	0.06	0.35	99.98	29.5
LC4	73.38	0.21	14.02	1.62	0.06	0.31	1.18	3.78	5.25	0.05	0.12	99.98	27.5
LC5	73.48	0.22	13.71	1.78	0.06	0.35	1.12	3.82	5.33	0.06	0.23	100.16	28.0
LC7	72.83	0.22	14.12	1.75	0.06	0.39	1.22	3.88	5.36	0.06	0.22	100.11	30.6
LC8	72.91	0.24	14.33	1.92	0.07	0.42	1.36	3.78	5.25	0.07	0.35	100.70	30.2
DD1	60.72	0.75	16.42	5.71	0.10	2.33	4.12	3.81	5.38	0.36	0.26	99.96	44.7
DD2	62.51	0.71	15.82	6.26	0.15	2.16	3.75	3.75	5.26	0.36	0.06	100.79	40.6
DD3	60.83	0.75	16.32	5.82	0.10	2.45	4.08	3.68	5.38	0.36	0.32	100.09	45.5
DD4	61.05	0.75	16.33	5.98	0.12	2.43	4.12	3.82	5.36	0.38	0.12	100.46	44.6
DD5	60.82	0.76	16.31	5.73	0.11	2.38	4.15	3.82	5.32	0.36	0.13	99.89	45.1
DD6	60.78	0.75	16.32	5.82	0.10	2.46	4.12	3.68	5.38	0.36	0.35	100.12	45.6
DD7	60.76	0.75	16.32	5.76	0.11	2.38	4.12	3.79	5.32	0.37	0.13	99.81	45.0
DD8	60.86	0.75	16.43	5.65	0.13	2.32	4.06	3.89	5.36	0.38	0.06	99.89	44.9
DD9	60.89	0.73	16.43	5.63	0.11	2.32	4.04	3.86	5.37	0.36	0.08	99.82	44.9
LST1	62.22	0.73	15.91	5.38	0.10	2.42	3.75	3.88	5.45	0.45	0.05	100.34	47.1
LST4	62.15	0.61	16.12	5.42	0.10	2.35	3.72	3.96	5.54	0.45	0.03	100.45	46.2
LST5	62.05	0.72	16.06	5.36	0.11	2.35	3.78	3.92	5.61	0.45	0.12	100.53	46.5
LST6	61.86	0.71	16.12	5.46	0.12	2.38	3.82	4.05	5.36	0.45	0.11	100.44	46.3
LST7	62.13	0.62	16.12	5.42	0.12	2.33	3.72	3.96	5.54	0.43	0.03	100.42	46.0
LST8	62.12	0.68	15.81	5.25	0.10	2.33	3.72	3.94	5.33	0.42	0.13	99.83	46.8
LST9	62.11	0.72	15.82	5.25	0.10	2.31	3.68	3.93	5.31	0.42	0.15	99.80	46.6
GSR-3	44.64	2.37	13.83	13.4	0.17	7.77	8.81	3.38	2.32	0.95	2.24	99.88	
GSR-3	44.75	2.36	14.14	13.35	0.16	7.74	8.82	3.18	2.30	0.97	2.12	99.89	
GSR-1	72.83	0.29	13.40	2.14	0.06	0.42	1.55	3.13	5.01	0.09	0.70	99.62	
GSR-1	72.65	0.29	13.52	2.18	0.06	0.46	1.56	3.15	5.03	0.11	0.69	99.70	

Values for GSR-1 and GSR-3 are from Wang et al. (2003)

complex and alkaline rocks are widespread in Sulu Orogenic Belt (Jiazishan, Jiaonan, Wulian, Juxian, Dadian, and Junan; Shandong Province Geology and Mineral Resources Bureau 1991; Han 2000). At present, investigation on some alkali rock mass (e.g., Jiaonan, Jiazishan, Juxian, Junan) has been carried out (215–115 Ma; Yang et al. 2005a; Zhang et al. 2005; Xie et al. 2006; Liu et al. 2006, 2008a; Wang et al. 2009; Chen and Jiang 2011). Nevertheless, a large number of controversies still exist for the alkaline rocks from the Sulu Orogenic Belt (e.g., the origin and evolution, the genetic mechanism, and tectonic implication).

The studied area is located in the central section of the Sulu Orogenic Belt from Jiaonan to Lashantou (Jiaonan, Liangcheng, Dadian, and Lanshantou; Fig. 1), and the alkaline rocks mainly include quartz-monzonites (JN1, JN2, JN3, JN4, JN5, JN6, JN7, JN8, DD1, DD2, DD3, DD4, DD5, DD6, DD7, DD8, DD9, LST1, LST4, LST5, LST6, LST7, LST8, LST9) from Jiaonan, Dadian, and Lanshantou, and the A-type granites (LC1, LC3, LC4, LC5, LC7, LC8) from Liangcheng.

Table 3 Trace element compositions (in ppm) of the alkaline rocks from from the Sulu Orogenic Belt, eastern NCC

Sample	JN1	JN2	JN3	JN4	JN5	JN6	JN7	JN8	LC1	LC3	LC4	LC5
V	99.4	103	108	106	106	84.5	89.6	99.4	16.8	15.5	12.4	14.2
Cr	27.6	24.6	33.2	31.8	32.5	32.5	33.6	30.6	11.8	13.2	19.3	33.6
Co	14.2	16.8	16.2	14.5	15.5	10.8	10.5	14.3	2.55	2.16	1.86	1.95
Ni	89.3	14.5	15.5	15.2	13.6	13.6	11.5	14.5	30.2	5.5	6.0	17.2
Ga	46.2	48.4	46.5	49.2	48.5	49.3	49.5	50.2	45.3	44.8	45.2	45.3
Rb	175	167	177	172	174	185	192	183	138	144	148	125
Sr	368	394	423	405	388	384	397	399	236	223	208	180
Y	23.3	23.5	24.9	24.0	24.9	25.6	25.8	24.7	18.4	17.7	15.0	14.3
Zr	365	288	348	285	301	374	266	233	240	245	250	239
Nb	19.2	16.8	17.2	19.1	18.1	20.5	18.6	19.1	17.1	15.3	11.3	13.5
Ba	1573	1609	1818	2475	2348	2085	2112	2365	839	914	1135	958
La	141	141	164	150	152	213	199	150	97	99	61	63
Ce	271	255	294	277	292	391	363	272	165	165	104	105
Pr	26.7	23.9	27.6	27.6	28.0	36.3	32.9	27.7	15.8	14.4	10.2	10.4
Nd	93.9	79.4	94.0	94.8	95.3	116.3	107	93.9	50.9	42.1	32.4	32.9
Sm	14.3	11.2	13.5	14.0	13.5	15.0	13.8	13.5	7.5	5.9	4.7	4.8
Eu	2.85	2.38	2.72	2.53	2.72	2.60	2.55	2.64	1.09	0.90	0.82	0.74
Gd	9.77	7.75	9.68	9.47	9.15	9.86	8.92	9.60	5.46	4.17	3.48	3.38
Tb	1.19	0.94	1.16	1.19	1.19	1.23	1.14	1.19	0.82	0.60	0.53	0.54
Dy	6.24	4.72	5.98	6.40	6.15	6.22	5.84	6.28	4.63	3.69	3.12	2.93
Ho	1.09	0.86	1.08	1.18	1.15	1.12	1.04	1.18	0.90	0.70	0.65	0.58
Er	3.15	2.51	3.07	3.40	3.27	3.40	3.15	3.40	2.73	2.17	1.93	1.80
Tm	0.44	0.33	0.42	0.48	0.44	0.44	0.44	0.46	0.39	0.32	0.29	0.28
Yb	2.86	2.37	2.72	3.07	2.89	3.10	2.80	3.05	2.68	2.24	1.99	1.91
Lu	0.42	0.41	0.41	0.46	0.44	0.48	0.44	0.46	0.43	0.35	0.32	0.30
Hf	11.1	8.01	8.76	8.35	8.83	10.2	8.15	7.25	6.89	6.83	6.67	6.52
Ta	0.46	0.35	0.35	0.38	0.35	0.43	0.41	0.36	0.38	0.35	0.28	0.32
Pb	24.6	26.6	26.5	31.4	27.5	28.5	28.8	25.8	25.3	24.5	23.6	20.5
Th	42.2	45.3	45.6	52.5	49.2	77.5	67.3	50.9	29.3	33.5	25.2	25.8
U	7.41	5.523	5.65	7.68	7.455	5.72	4.46	6.89	3.00	3.13	2.69	2.77
(La/Yb)N	33.2	40.1	40.6	33.0	35.4	46.4	47.8	33.3	24.4	29.8	20.6	22.1
Eu/Eu*	0.70	0.74	0.70	0.64	0.71	0.61	0.66	0.67	0.50	0.53	0.59	0.53
TZr (°C)	873	860	875	857	860	887	851	830	869	871	874	868

LC7	LC8	DD1	DD2	DD3	DD4	DD5	DD6	DD7	DD8	DD9	LST1	LST4
16.8	13.6	108	108	107	103	106	108	112	108	108	103	99.8
11.8	10.3	35.5	30.3	31.8	54.6	29.3	15.5	38.1	29.7	31.8	73.8	58.5
2.53	1.86	14.5	14.6	14.5	14.5	14.6	14.5	14.6	14.5	14.5	14.5	14.5
29.8	3.7	16.3	14.1	15.2	25.6	13.5	16.5	19.2	14.2	15.3	21.3	20.5
44.6	45.3	49.3	49.8	48.6	48.9	49.2	49.5	49.5	49.8	48.9	47.6	47.8
138	169	188	178	173	196	186	186	194	183	174	206	208
236	232	329	336	352	340	333	308	293	325	298	473	496
18.3	16.4	28.1	28.3	28.2	28.8	28.3	28.4	28.3	27.7	27.9	28.9	22.7
241	249	286	265	315	293	268	295	256	253	282	398	377
11.0	11.8	19.1	18.2	19.4	22.2	18.6	19.3	19.2	18.2	19.3	19.8	15.8
1045	1052	1243	1265	1368	2068	2482	2316	2225	2391	2473	2264	2327
97	66	165	150	150	161	158	167	181	150	152	146	133
165	115	312	284	275	293	306	312	333	284	280	272	240
15.8	11.5	29.8	27.6	27.6	28.9	29.0	29.9	31.6	27.6	27.6	27.1	23.9

Table 3 continued

LC7	LC8	DD1	DD2	DD3	DD4	DD5	DD6	DD7	DD8	DD9	LST1	LST4
50.9	37.0	101.2	95.3	94.6	96.6	99.3	101.2	106	95.3	94.8	93.3	84.0
7.5	5.6	14.3	14.3	14.3	13.8	14.4	14.3	15.5	14.3	14.3	13.5	12.6
1.09	0.93	2.74	2.70	2.57	2.38	2.80	2.74	2.80	2.69	2.56	2.85	2.69
5.44	4.31	10.28	9.64	9.48	9.14	10.3	10.3	10.1	9.65	9.48	9.55	8.76
0.82	0.60	1.28	1.21	1.19	1.19	1.28	1.23	1.29	1.21	1.19	1.19	1.08
4.63	3.59	6.54	6.35	6.40	6.22	6.53	6.54	6.86	6.35	6.40	6.22	5.53
0.90	0.67	1.21	1.17	1.18	1.17	1.22	1.21	1.22	1.17	1.18	1.09	0.99
2.73	2.18	3.49	3.34	3.40	3.38	3.57	3.49	3.69	3.36	3.40	3.21	2.83
0.41	0.32	0.48	0.46	0.48	0.48	0.48	0.48	0.48	0.46	0.48	0.43	0.39
2.68	2.07	3.15	3.11	3.09	3.23	3.15	3.15	3.17	3.11	3.10	2.78	2.41
0.44	0.32	0.48	0.46	0.46	0.53	0.48	0.47	0.48	0.46	0.46	0.42	0.35
6.98	6.74	8.01	8.16	8.53	8.13	8.23	7.91	7.82	7.91	7.97	10.9	11.4
0.38	0.28	0.36	0.36	0.38	0.52	0.36	0.36	0.36	0.38	0.38	0.42	0.32
25.4	23.3	29.4	38.4	31.4	28.4	29.8	29.2	28.5	38.4	31.4	25.3	24.8
29.3	39.6	54.2	50.6	52.6	60.8	48.8	54.5	56.4	50.6	52.6	47.8	44.9
3.00	2.55	7.10	7.06	6.62	6.91	7.18	6.47	5.38	6.15	7.68	4.36	3.46
24.4	21.6	35.3	32.6	32.9	33.5	33.9	35.9	38.4	32.6	33.0	35.5	37.3
0.50	0.55	0.66	0.67	0.64	0.61	0.67	0.66	0.64	0.66	0.63	0.73	0.74
869	873	857	853	868	859	850	861	846	845	856	892	887

LST5	LST6	LST7	LST8	LST9	OU-6 (RV*)	OU-6 (MV*)	GBPG-1 (RV*)	GBPG-1 (MV*)
97.5	105	112	103	96.8	129	131	96.5	103
30.2	30.3	93.3	37.3	30.3	70.8	73.5	181	187
14.1	15.3	15.8	14.2	14.6	29.1	30.3	19.5	20.2
15.2	16.8	18.5	20.3	17.5	39.8	42.5	59.6	60.6
48.6	49.3	48.8	48.5	48.7	24.3	26.5	18.6	20.9
212	209	208	207	203	120	122	56.2	61.4
509	471	515	477	494	131	136	364	377
23.0	22.6	22.2	22.5	22.8	27.4	26.2	18.0	17.2
379	366	386	379	400	174	183	332	224
17.3	17.5	16.8	18.3	18.5	14.8	15.3	9.93	8.74
2278	2411	2544	2488	2348	477	486	908	921
165	154	148	141	150	33.0	33.1	53.0	51.0
280	285	272	261	259	74.4	78.0	103	105
27.5	27.7	26.7	26.3	24.7	7.8	8.1	11.5	11.6
93.5	94.0	91.9	91.6	83.0	29	30.6	43.3	42.4
13.1	13.1	13.8	13.5	12.0	5.92	5.99	6.79	6.63
2.64	2.60	2.76	2.60	2.47	1.36	1.35	1.79	1.69
9.15	8.89	9.55	9.59	8.17	5.27	5.5	4.74	4.47
1.14	1.11	1.19	1.14	1.03	0.85	0.83	0.60	0.59
5.64	5.69	5.77	5.86	5.22	4.99	5.06	3.26	3.17
0.99	0.99	1.08	1.07	0.95	1.01	1.02	0.69	0.66
2.87	2.97	2.96	3.06	2.70	2.98	3.07	2.01	2.02
0.39	0.38	0.42	0.42	0.36	0.44	0.46	0.30	0.29
2.41	2.41	2.56	2.62	2.41	3.00	3.09	2.03	2.03
0.33	0.35	0.41	0.42	0.35	0.45	0.47	0.31	0.31
10.8	11.3	11.1	11.0	11.2	4.70	4.86	6.07	5.93
0.38	0.33	0.35	0.35	0.32	1.06	1.02	0.40	0.46

Table 3 continued

LST5	LST6	LST7	LST8	LST9	OU-6 (RV*)	OU-6 (MV*)	GBPG-1 (RV*)	GBPG-1 (MV*)
23.8	24.4	27.4	25.4	34.2	28.2	32.7	14.1	14.5
45.6	49.6	46.2	45.7	44.7	11.5	13.9	11.2	11.4
4.62	5.25	5.43	4.54	4.03	1.96	2.19	0.90	0.99
46.1	43.2	39.0	36.4	42.1				
0.70	0.70	0.70	0.66	0.72				
886	883	890	887	907				

Values for GBPG-1 and OU-6 are from Thompson et al. (2000) and Potts and Kane (2005), respectively

2.1 Jiaonan quartz-monzonites

The Jiaonan quartz monzonitic intrusion ($\sim$ 390 km^2) mainly intruded into Archean or lower Proterozoic gneisses and is the largest intrusion in the study area. It is associated with the Yanshanian granites (Fig. 1). These alkaline rocks are light grey and characteristically medium- to coarse-grained with granular and porphyritic textures. They are dominated by K-feldspar (40 %–43 %), quartz (11.0 %–14.0 %), andesine (30 %–33 %), minor amphibole, and biotite (2.0 %–4.0 %). Accessory minerals include apatite, zircon, magnetite, and titanite.

2.2 Dadian quartz-monzonites

Dadian A-type granites outcrop over ca. 180 km^2; these alkaline rocks also intruded into the Archean or lower Proterozoic gneisses and were intruded by the Yanshanian granite (Fig. 1). The rocks are commonly light grey, medium- to coarse-grained with granular and porphyritic textures. In addition, the Dadian A-type granites consist predominantly of K-feldspar (40 %–45 %), quartz (10.0 %–14.0 %), andesine (32 %–34 %), diopside (8.0 %–9.0 %), subordinate ($\sim$ 2.0 %–3.0 %) amphibole and biotite, and accessory minerals including apatite, zircon, magnetite, and titanite.

2.3 Lanshantou quartz-monzonites

The Lanshantou A-type granitic intrusion ($\sim$ 160 km^2) mainly intruded into Archean or lower Proterozoic gneisses. They are light grey and characteristically medium- to coarse-grained with granular and porphyritic textures. Furthermore, these alkaline rocks are dominated by K-feldspar (40 %–44 %), quartz (10.0 %–15.0 %), andesine (30 %–35 %), diopside (8.0 %–10.0 %), subordinate ($\sim$ 2.0 %) amphibole and biotite, and accessory minerals including apatite, zircon, magnetite, and titanite.

2.4 Liangcheng A-type granites

The Liangcheng A-type granites ($\sim$ 85 km^2) also intruded into Archean or lower Proterozoic gneisses (Fig. 1). These alkaline rocks are commonly light grey to pink in color and composed of quartz (25 %–33 %), perthite (30 %–45 %), albite (An 0-5) (15.0 %–20 %), and minor muscovite. Accessory minerals include zircon, magnetite, and apatite.

3 Analytical procedures

Thirty samples from the alkaline rocks were collected for this study (Fig. 1). Zircon grains were separated from four samples (JN02, LC01, DD02, and LST01) using conventional heavy liquid and magnetic techniques at the Langfang Regional Geological Survey, Hebei Province, China. After separation and mounting, the morphology and internal structure of the zircon were imaged using transmitted and reflected light and by cathodoluminescence (CL) techniques at the State Key Laboratory of Continental Dynamics, Northwest University (Fig. 2). Prior to zircon U–Pb dating, grain mount surfaces were washed in dilute HNO_3 and pure alcohol to remove any potential lead contamination. Zircon U–Pb and $^{207}Pb/^{206}Pb$ weighted average ages were determined by LA-ICP-MS (Table 1; Fig. 2) using an Agilent 7500a ICP-MS instrument equipped with a 193 nm excimer laser at the State Key Laboratory of Continental Dynamics, Northwest University. The zircon standard 91500 was used for quality control, and a NIST 610 standard was used for data optimization. A spot diameter of 24 μm was used during analysis, employing the methodologies described by Liu et al. (2010a, b, c). Common Pb correction was undertaken following the approach of Andersen (2002), and the resulting data were processed using GLITTER and ISOPLOT (Table 1; Fig. 2). Uncertainties on individual LA-ICP-MS analyses are quoted at the 95 % (1σ) confidence level.

Major oxides were analyzed with a PANalytical Axios-advance X-ray fluorescence spectrometer (XRF) at the

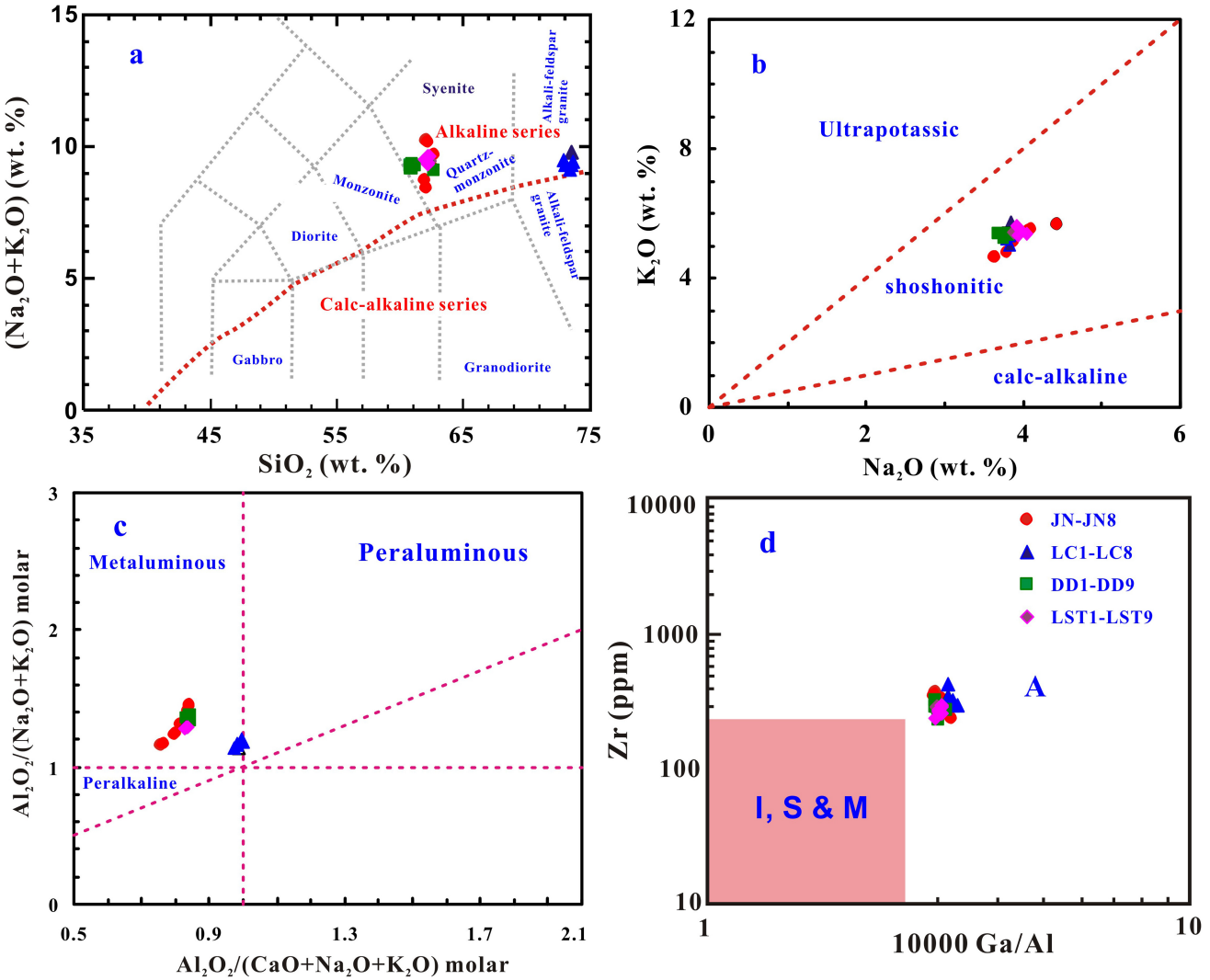

Fig. 3 Classification of the quartz monzonites and A-type granites from the Sulu Orogenic Belt on the basis of **a** the TAS diagram. All the major element data have been recalculated to 100% on a LOI-free basis (Middlemost 1994; Le Maitre 2002); **b** Na_2O versus K_2O diagram, showing the alkaline rocks to be shoshonitic (Middlemost 1972); **c** $Al_2O_3/(Na_2O + K_2O)$ molar versus $Al_2O_3/(CaO + Na_2O + K_2O)$molar plot. Most samples fall in the metaluminous field except some A-type granites straddle the metaluminous and peralkaline boundary; **d** (10000) * Ga/Al versus Zr plot, all the sample fall in the A-type field. Legends in other figures are the same as in this figure

State Key Laboratory of Ore Deposit Geochemistry (LODG), Institute of Geochemistry, Chinese Academy of Sciences. Fused glass disks were used and the analytical precision as determined on the Chinese National standard GSR-3 was better than 5.0 % (Table 2). Loss on ignition was obtained using 1.0 g powder heated up to 1100 °C for 1 h. Trace elements were performed with an ELAN 6000 ICP-MS at the LODG, following procedures described by Qi et al. (2000). The discrepancy between triplicate analyses is less than 5.0 % for all elements. Analyses of international standards OU-6 and GBPG-1 are in good agreement with recommended values (Table 3).

For Rb–Sr and Sm–Nd isotope analyses, sample powders were spiked with mixed isotope tracers, dissolved in Teflon capsules with HF + HNO_3 acids, and separated by conventional cation-exchange technique (Zhang et al. 2001). Isotopic measurements were performed using a Finnigan Triton Ti thermal ionization mass spectrometer at the LODG. Procedural blanks yielded concentrations of < 200 pg for Sm and Nd and < 500 pg for Rb and Sr, and mass fractionation corrections for Sr and Nd isotopic ratios were based on $^{86}Sr/^{88}Sr = 0.1194$ and $^{146}Nd/^{144}Nd = 0.7219$, respectively. Analysis of the NBS987 and La Jolla standards yielded values of $^{87}Sr/^{86}Sr = 0.710246 \pm 16$ (2σ), and $^{143}Nd/^{144}Nd = 0.511863 \pm 8$ (2σ), respectively.

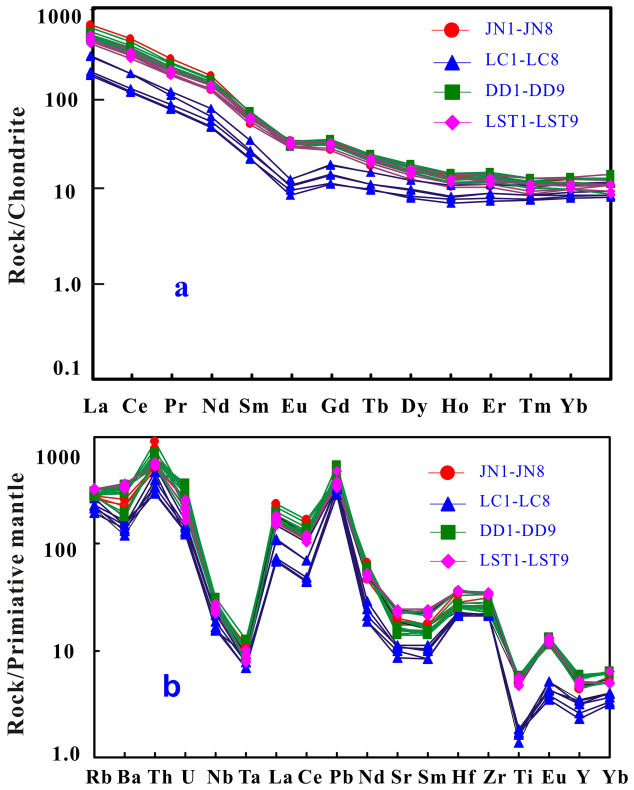

Fig. 4 Chondrite-normalized REE and **b** Primitive mantle-normalized multi-element variation diagrams for the alkaline rocks from the Sulu Orogenic Belt, eastern NCC. Concentrations are normalized to chondrite composition of Sun and McDonough (1989)

In-situ zircon Hf isotopic analyses were performed on a Nu Plasma HR MC-ICP-MS equipped with a GeoLas 2005 193 nm ArF-excimer laser-ablation system. Analyses were carried out using a spot size of 44 μm and He was also used as a carrier gas. The laser repetition rate is 10 Hz and the energy density applied is 15–20 J/cm^{-2}. During the analysis, the $^{176}Hf/^{177}Hf$ ratio of the standard zircon (91500) was 0.282295 ± 0.000027 (n = 14, 2σ), which is in good agreement with the recommended $^{176}Hf/^{177}Hf$ ratio within 2σ (0.2823075 ± 58, 2σ; 0.282015 ± 0.000029, 2σ) (Griffin et al. 2006; Wu et al. 2006). All the above analysis was performed at the Key state Laboratory of Continental Dynamics, Northwest University, Xi'an, China.

4 Results

4.1 Zircon U–Pb ages

Euhedral zircons in samples JN02, LC01, DD02, and LST01 are clean and prismatic and show clear oscillatory magmatic zoning (Fig. 2). Fourteen zircon grains from sample JN02 yielded a weighted mean $^{206}Pb/^{238}U$ age of 121.3 ± 5.7 Ma (1σ, 95 % confidence interval; Table 1; Fig. 2a). Thirteen zircon grains from sample LC01 yielded a weighted mean $^{206}Pb/^{238}U$ age of 123.0 ± 1.2 Ma (1σ; 95 % confidence interval; Table 1; Fig. 2b). Twelve zircon grains from sample DD02 yielded a weighted mean $^{206}Pb/^{238}U$ age of 127.1 ± 2.4 Ma (1σ; 95 % confidence interval; Table 1; Fig. 2c). Thirteen zircon grains from sample LST01 yielded a weighted mean $^{206}Pb/^{238}U$ age of 119.5 ± 4.8 Ma (1σ; 95 % confidence interval; Table 2; Fig. 2d). These new-age data provide the best estimates of the crystallization ages of alkaline rocks within the study area. No major zircon inheritance was observed in any of the samples.

4.2 Major and trace element geochemistry

Geochemical data for the A-type granites from Sulu Orogenic Belt are listed in Tables 2 and 3. The alkaline rocks have a wide range of chemical compositions, with SiO_2 = 60.76–73.48 wt %, TiO_2 = 0.18–0.76 wt %, Al_2O_3 = 13.71–16.43 wt %, Fe_2O_3 = 1.58–6.26 wt %, MnO = 0.06–0.15 wt %, MgO = 0.31–2.75 wt %, CaO = 1.08–4.42 wt %, Na_2O = 3.63–4.43 wt %, K_2O = 4.68–5.71 wt %, and P_2O_5 = 0.05–0.51 wt %. These rocks are relatively high in total alkalis, with $K_2O + Na_2O$ range from 8.32 to 10.11 wt%. All alkaline rocks plot in the alkaline field on the total alkali-silicon (TAS) diagram (Fig. 3a). All samples straddle the shoshonitic series in the Na_2O versus K_2O (Fig. 3b). In a plot of molar ratios of $Al_2O_3/(Na_2O + K_2O)$ and $Al_2O_3/(CaO + Na_2O + K_2O)$, the alkaline rocks are all metaluminous (Fig. 3c). In addition, the 10,000 × Ga/Al ratios of the A-type granites range from 2.75 to 3.45. In the Ga/Al versus Zr discrimination diagram (Fig. 3d) of Whalen et al. (1987), the felsic rocks are all classified as A-type granite. The A-type granites display an inconspicuous correlation between MgO, Al_2O_3, Fe_2O_3, CaO, TiO_2, P_2O_5, Zr, Sr, Ba, and SiO_2 Na_2O, K_2O, and Rb (not shown).

The A-type granites are all characterized by LREE enrichment and HREE depletion, with a wide range $(La/Yb)_N$ values (20–48) and moderate negative Eu anomalies (Eu/Eu* = 0.50–0.74) (Fig. 4a). In the primitive mantle-normalized trace element diagrams, the A-type granites show enrichment in LILEs (i.e., Rb, Th, U, and Pb) and depletion in Ba, Sr and REEs (i.e., Nb, Ta, and Ti) (Fig. 4b).

4.3 Sr–Nd–Pb isotopes

Sr, Nd, and Pb isotopes for the A-type granites from Sulu Orogenic Belt are listed in Tables 4 and 5. The studied alkaline rocks show very uniform $(^{87}Sr/^{86}Sr)_i$ ranging from

Table 4 Sr-Nd isotopic compositions of the alkaline rocks from the Sulu Orogenic Belt, eastern NCC

Sample	Age (Ma)	Rb (ppm)	Sr (ppm)	$^{87}Rb/^{86}Sr$	$^{87}Sr/^{86}Sr$	± 2σ	Sm (ppm)	Nd (ppm)	$^{147}Sm/^{144}Nd$	$^{143}Nd/^{144}Nd$	± 2σ	$(^{87}Sr/^{86}Sr)i$	$(^{143}Nd/^{144}Nd)i$	$\varepsilon_{Nd}(t)$
JN1	121.3	115	1132	0.294	0.708955	12	10.4	72.5	0.086	0.511653	9	0.708448	0.511584	− 17.5
JN2	121.3	125	1165	0.311	0.709033	13	10.6	68.3	0.094	0.511652	10	0.708497	0.511578	− 17.6
JN5	121.3	136	1072	0.367	0.709063	14	11.3	73.8	0.092	0.511648	10	0.708430	0.511575	− 17.7
JN6	121.3	134	1065	0.364	0.709074	13	11.5	76.2	0.091	0.511651	10	0.708446	0.511579	− 17.6
JN7	121.3	122	1161	0.304	0.709005	14	10.5	66.4	0.096	0.511649	8	0.708480	0.511573	− 17.7
JN8	121.3	119	1153	0.299	0.708984	11	11.7	83.5	0.085	0.511644	12	0.708469	0.511576	− 17.6
LC1	123.0	138	236	1.693	0.711508	12	5.98	40.5	0.089	0.511572	10	0.708548	0.511500	− 19.1
LC3	123.0	116	143	2.349	0.712655	13	3.43	23.6	0.088	0.511563	10	0.708549	0.511492	− 19.3
LC5	123.0	153	215	2.061	0.712148	12	3.75	25.2	0.090	0.511557	10	0.708546	0.511484	− 19.4
LC8	123.0	126	148	2.465	0.712853	13	5.51	36.4	0.092	0.511564	9	0.708544	0.511488	− 19.3
DD1	127.1	186	812	0.663	0.709305	12	11.4	78.8	0.0871	0.511648	9	0.708107	0.511576	− 17.5
DD3	127.1	175	846	0.599	0.709308	14	11.4	75.3	0.092	0.511645	9	0.708226	0.511569	− 17.7
DD4	127.1	173	865	0.579	0.709293	13	10.8	74.5	0.088	0.511648	8	0.708247	0.511575	− 17.5
DD5	127.1	168	858	0.567	0.709201	12	11.2	74.2	0.091	0.511646	10	0.708177	0.511570	− 17.6
DD9	127.1	184	864	0.617	0.709244	14	12.5	83.6	0.090	0.511662	9	0.708130	0.511591	− 17.4
LST1	119.5	135	1025	0.381	0.709515	12	4.03	20.4	0.119	0.511716	9	0.708867	0.511623	− 16.8
LST5	119.5	131	1006	0.377	0.709465	10	4.27	21.3	0.121	0.511719	9	0.708825	0.511624	− 16.8
LST6	119.5	128	1023	0.362	0.709436	14	4.43	21.6	0.1240	0.511721	7	0.708821	0.511624	− 16.8
LST8	119.5	136	1012	0.389	0.709478	13	5.24	23.7	0.134	0.511758	10	0.708817	0.511758	− 17.2

The compositions were calculated using Chondrite Uniform Reservoir values and decay constants of $\lambda_{Rb} = 1.42 \times 10^{-11}$ year^{-1} (Steiger and Jäger 1977) and $\lambda_{Sm} = 6.54 \times 10^{-12}$ year^{-1} (Lugmair and Harti 1978)

Table 5 Pb isotopic compositions of the alkaline rocks from the Sulu Orogenic Belt, eastern NCC

Sample	Age (Ma)	$^{206}Pb/^{204}Pb$	$^{207}Pb/^{204}Pb$	$^{208}Pb/^{204}Pb$	U (ppm)	Pb (ppm)	Th (ppm)	$^{238}U/^{204}Pb$	$^{235}U/^{204}Pb$	$^{232}Th/^{204}Pb$	$(^{206}Pb/^{204}Pb)i$	$(^{207}Pb/^{204}Pb)i$	$(^{208}Pb/^{204}Pb)i$
JN1	121.3	16.9246	15.385	37.611	1.75	47.6	8.26	2.2	0.0163	11.0	16.882	15.383	37.545
JN2	121.3	16.965	15.3862	37.711	1.62	22.3	4.65	4.5	0.0323	13.2	16.880	15.382	37.631
JN5	121.3	16.9741	15.428	37.823	1.66	21.4	5.35	4.8	0.0345	15.9	16.883	15.424	37.727
JN6	121.3	16.923	15.383	37.671	1.25	38.2	4.27	2.0	0.0145	7.1	16.885	15.381	37.628
JN7	121.3	16.925	15.421	37.672	1.32	37.5	4.16	2.2	0.0156	7.0	16.884	15.419	37.630
JN8	121.3	16.934	15.423	37.678	1.44	35.2	4.25	2.5	0.0182	7.6	16.886	15.421	37.631
LC1	123.0	16.834	15.479	37.715	1.37	19.4	12.2	4.3	0.0313	39.7	16.751	15.475	37.472
LC3	123.0	16.837	15.478	37.705	1.48	20.8	12.5	4.3	0.0315	37.9	16.753	15.474	37.472
LC5	123.0	16.893	15.483	37.691	2.19	18.6	10.4	7.2	0.0522	35.3	16.754	15.476	37.474
LC8	123.0	16.811	15.479	37.616	2.21	45.3	16.2	3.0	0.0216	22.6	16.751	15.476	37.473
DD1	127.1	16.997	15.447	37.982	2.36	46.5	16.9	3.1	0.0227	23.1	16.935	15.444	37.836
DD3	127.1	16.991	15.449	37.971	2.31	46.4	15.3	3.1	0.0222	21.0	16.930	15.446	37.838
DD4	127.1	16.978	15.447	37.915	1.68	47.2	9.41	2.2	0.0159	12.7	16.934	15.445	37.835
DD5	127.1	17.036	15.451	37.957	1.76	20.5	6.35	5.3	0.0383	19.7	16.930	15.446	37.832
DD9	127.1	16.974	15.446	37.914	1.54	45.3	9.26	2.1	0.0152	13.0	16.935	15.444	37.837
LST1	119.5	16.983	15.436	37.943	2.38	46.4	13.3	3.2	0.0229	18.2	16.924	15.433	37.835
LST5	119.5	17.006	15.437	37.955	2.65	38.1	12.4	4.3	0.0310	20.7	16.926	15.433	37.832
LST6	119.5	17.045	15.441	38.036	2.46	23.2	12.4	6.5	0.0473	34.0	16.922	15.435	37.834
LST8	119.5	16.923	15.535	37.836	1.15	16.5	5.61	4.3	0.0311	21.6	16.923	15.535	37.836

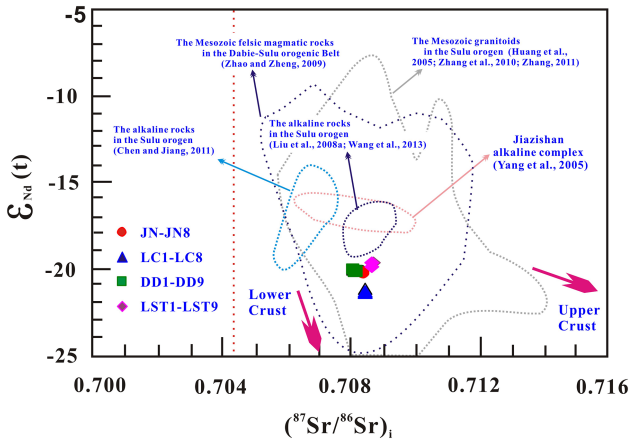

Fig. 5 Variations in initial $^{87}Sr/^{86}Sr$ versus ε_{Nd} (t) values for the alkaline rocks from the Sulu Orogenic Belt, eastern NCC. The studied rocks analyzed during this study plot within the enriched mantle source field

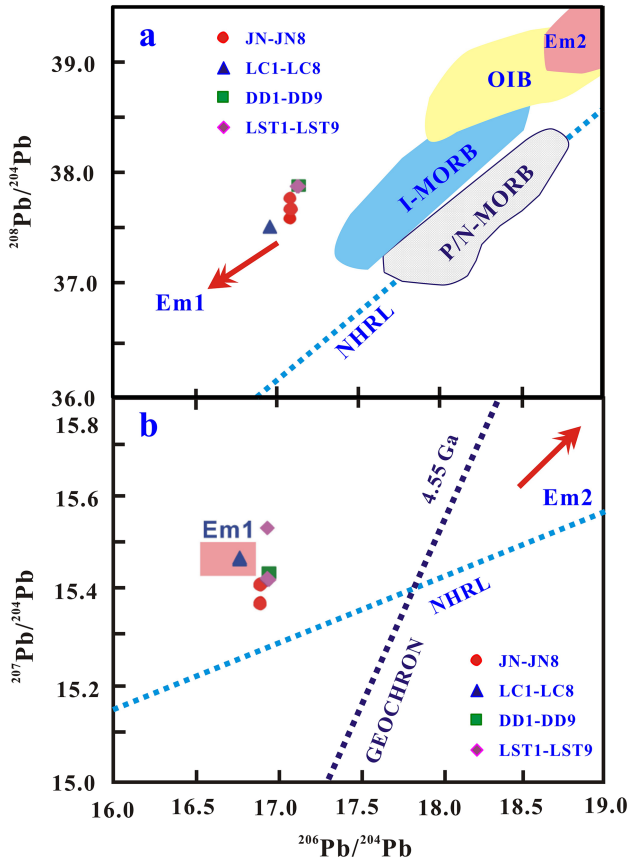

Fig. 6 $^{208}Pb/^{204}Pb$ and $^{207}Pb/^{204}Pb$ versus $^{206}Pb/^{204}Pb$ diagrams for the alkaline rocks. Fields for I-MORB (Indian MORB) and P&N-MORB (Pacific and North Atlantic MORB), OIB, NHRL and 4.55 Ga geochron are after Barry and Kent 1998; Zou et al. 2000), and Hart (1984), respectively

0.708 to 0.7089 and relatively small variation in initial ε_{Nd} (t) values from − 19.4 to − 16.8, which suggests a common source region. In addition, the Sr–Nd isotopic compositions (Fig. 5) are comparable to those of the Mesozoic medium-acid rocks, granitoids, gabbros, lamprophyres, adakites, and alkaline rocks in Sulu-Dabie Orogenic Belt (Zhao et al. 1997; Zhou and Lu 2000; Fan et al. 2001; Zhang et al. 2005; Meng et al. 2005; Huang et al. 2005; Yang et al. 2005a; Liu 2004; Liu et al. 2005a, b, 2006, 2008a, 2009, 2011, 2012a, b, 2013a, b, c, d, 2014; Zhang et al. 2010; Chen and Jiang 2011; Wang et al. 2013). The Pb isotopic ratios in the alkaline rocks are characterized by $^{206}Pb/^{204}Pb$ = 16.751–16.935, $^{207}Pb/^{204}Pb$ = 15.381–15.535, $^{208}Pb/^{204}Pb$ = 37.472–37.838 (Table 5). They are significantly different from those of the Yangtze lithospheric mantle (($^{206}Pb/^{204}Pb$ = 17.649–18.603, $^{207}Pb/^{204}Pb$ = 15.422–15.623, $^{208}Pb/^{204}Pb$ = 37.674–38.521; Chen et al. 2001; Yan et al. 2003, 2005; Yang et al. 2004; Wang et al. 2005) and are identical to those of alkaline complex and mafic rocks from the central NCC and Sulu-Dabie Orogen ($^{206}Pb/^{204}Pb < 17.5$; Yan et al. 2003; Zhang et al. 2004; Xie et al. 2006), having a clear EM1 affinity (Fig. 6).

4.4 Zircon Hf isotopes

Zircon Hf isotope results are listed in Table 6. Nineteen spot analyses were obtained for sample JN02, yielding relatively uniform ε_{Hf} (t) values of between − 21.8 and − 25.7, corresponding to T_{DM2} model ages of between 2652 and 2792 Ma (Table 6; Figs. 7, 8, 9), and giving an average of ε_{Hf} (t) = − 23.9 and T_{DM2} = 2683 Ma. Twenty spot analyses were obtained for sample LC01; they show a narrow range of ε_{Hf} (t) values − 23.4 and − 24.3, corresponding to T_{DM2} model ages between 2632 and 2684 Ma (Table 6; Figs. 7, 8, 9), and yielded a mean ε_{Hf} (t) = − 23.7 and T_{DM2} = 2668 Ma. Nineteen spot analyses were obtained for sample DD02. The determined ε_{Hf} (t) values vary between − 21.3 and − 22.4, corresponding to T_{DM2} model ages in the range from 2525 Ma and 2595 Ma (Table 6; Figs. 7, 8, 9). These nineteen spots gave a mean ε_{Hf} (t) = − 21.9 and T_{DM2} = 2562 Ma. Nineteen spot analyses were obtained for sample LST01, giving ε_{Hf} (t) values between − 21.1 and − 25.5, corresponding to T_{DM2} model ages between 2504 and 2595 Ma (Table 6; Figs. 7, 8, 9), thus yielding an average of ε_{Hf} (t) = − 22.0 and T_{DM2} = 565 Ma.

5 Discussion

5.1 Source, fractional crystallization, and crustal assimilation

The studied alkaline rocks are characterized by similar patterns of rare earth and trace elements (Table 3; Fig. 4a,

Table 6 Hf isotopic compositions of representative alkaline samples in the the Sulu Orogenic Belt, eastern NCC

Spot	$^{176}Yb/^{177}Hf$	$^{176}Lu/^{177}Hf$	$^{176}Hf/^{177}Hf$	2σ	ε_{Hf} (t)	T_{DM1} (Ma)	T_{DM2} (Ma)	$f_{Lu/Hf}$
JN02								
1	0.029586	0.000964	0.281993	0.000016	− 25.0	1771	2749	− 0.97
2	0.052717	0.001625	0.282003	0.000018	− 24.7	1788	2730	− 0.95
3	0.098563	0.002924	0.282086	0.000019	− 21.8	1731	2552	− 0.93
4	0.059815	0.001915	0.281975	0.000018	− 25.7	1842	2792	− 0.94
5	0.034469	0.001118	0.282003	0.000017	− 24.6	1764	2727	− 0.97
6	0.063329	0.001972	0.282027	0.000015	− 23.9	1771	2678	− 0.94
7	0.046168	0.001496	0.282011	0.000017	− 24.4	1771	2711	− 0.95
8	0.038843	0.001332	0.282034	0.000018	− 23.6	1731	2660	− 0.96
9	0.050533	0.001683	0.282064	0.000018	− 22.5	1705	2595	− 0.95
10	0.064315	0.002143	0.282033	0.000016	− 23.7	1770	2665	− 0.94
11	0.032746	0.001257	0.282031	0.000016	− 23.7	1731	2666	− 0.96
12	0.045333	0.001536	0.282024	0.000015	− 23.9	1754	2683	− 0.95
13	0.063869	0.002204	0.282013	0.000016	− 24.4	1802	2710	− 0.94
14	0.056225	0.001562	0.282024	0.000016	− 23.9	1755	2683	− 0.95
15	0.058065	0.001561	0.282034	0.000018	− 23.6	1741	2661	− 0.95
16	0.042815	0.001208	0.282036	0.000019	− 23.5	1722	2655	− 0.96
17	0.043579	0.001295	0.282023	0.000015	− 23.9	1745	2684	− 0.96
18	0.055138	0.001481	0.282015	0.000016	− 24.2	1764	2702	− 0.96
19	0.036295	0.000983	0.282031	0.000016	− 23.6	1719	2665	− 0.97
LC01								
1	0.037236	0.000994	0.282037	0.000019	− 23.4	1712	2652	− 0.97
2	0.047835	0.001377	0.282013	0.000016	− 24.3	1763	2706	− 0.96
3	0.045227	0.001318	0.282026	0.000020	− 23.8	1741	2676	− 0.96
4	0.027637	0.000774	0.282022	0.000015	− 23.9	1722	2683	− 0.98
5	0.038285	0.001162	0.282042	0.000018	− 23.2	1712	2641	− 0.97
6	0.040084	0.001056	0.282037	0.000017	− 23.4	1715	2652	− 0.97
7	0.055067	0.001479	0.282039	0.000016	− 23.4	1730	2648	− 0.96
8	0.038793	0.001336	0.282036	0.000017	− 23.4	1728	2654	− 0.96
9	0.050527	0.001679	0.282047	0.000018	− 23.1	1728	2632	− 0.95
10	0.06435	0.002146	0.282036	0.000016	− 23.5	1766	2658	− 0.94
11	0.032754	0.001261	0.282029	0.000016	− 23.7	1734	2670	− 0.96
12	0.045338	0.001543	0.282027	0.000017	− 23.8	1750	2675	− 0.95
13	0.063874	0.002207	0.282015	0.000016	− 24.3	1799	2704	− 0.93
14	0.056235	0.001559	0.282026	0.000016	− 23.8	1752	2677	− 0.95
15	0.058076	0.001564	0.282038	0.000018	− 23.4	1736	2651	− 0.95
16	0.042842	0.001211	0.282038	0.000019	− 23.4	1720	2650	− 0.96
17	0.043586	0.001285	0.282026	0.000016	− 23.8	1740	2677	− 0.96
18	0.055144	0.001485	0.282023	0.000016	− 23.9	1753	2684	− 0.96
19	0.036295	0.001332	0.282034	0.000016	− 23.5	1731	2659	− 0.96
20	0.044775	0.001286	0.282014	0.000018	− 24.2	1757	2704	− 0.96
DD02								
1	0.027363	0.000784	0.282073	0.000018	− 22.0	1652	2568	− 0.98
2	0.036883	0.001106	0.282081	0.000015	− 21.7	1654	2551	− 0.97
3	0.048760	0.001306	0.282092	0.000020	− 21.4	1649	2529	− 0.96
4	0.018478	0.000564	0.282085	0.000016	− 21.6	1626	2540	− 0.98
5	0.054609	0.001574	0.282071	0.000016	− 22.1	1690	2576	− 0.95
6	0.036307	0.001058	0.282085	0.000016	− 21.6	1648	2543	− 0.97

Table 6 continued

Spot	$^{176}Yb/^{177}Hf$	$^{176}Lu/^{177}Hf$	$^{176}Hf/^{177}Hf$	2σ	ε_{Hf} (t)	T_{DM1} (Ma)	T_{DM2} (Ma)	$f_{Lu/Hf}$
7	0.036924	0.001042	0.282093	0.000014	− 1.3	1636	2525	− 0.97
8	0.068916	0.001931	0.282084	0.000016	− 21.7	1688	2549	− 0.94
9	0.023981	0.000728	0.282083	0.000014	− 21.6	1636	2545	− 0.98
10	0.060873	0.001688	0.282091	0.000018	− 21.4	1666	2531	− 0.95
11	0.017424	0.000518	0.282061	0.000014	− 22.4	1657	2593	− 0.98
12	0.046217	0.001325	0.282062	0.000019	− 22.4	1692	2595	− 0.96
13	0.044683	0.001348	0.282065	0.000018	− 22.3	1688	2588	− 0.96
14	0.044962	0.001336	0.282068	0.000018	− 22.2	1684	2582	− 0.96
15	0.017465	0.000476	0.282073	0.000020	− 22.0	1639	2566	− 0.99
16	0.056252	0.001493	0.282082	0.000015	− 21.8	1671	2552	− 0.96
17	0.043658	0.001294	0.282066	0.000016	− 22.4	1684	2588	− 0.96
18	0.055181	0.001496	0.282075	0.000016	− 22.1	1681	2569	− 0.95
19	0.036246	0.001354	0.282068	0.000016	− 22.3	1684	2584	− 0.96
LST01								
1	0.001814	0.000851	0.282104	0.000014	− 21.1	1612	2504	− 0.97
2	0.001977	0.000832	0.282092	0.000016	− 21.5	1628	2531	− 0.96
3	0.002215	0.000745	0.282082	0.000014	− 21.8	1638	2552	− 0.98
4	0.001867	0.000904	0.282093	0.000018	− 21.5	1629	2529	− 0.97
5	0.001569	0.000685	0.282064	0.000016	− 22.5	1660	2591	− 0.98
6	0.004118	0.000744	0.282063	0.000016	− 22.5	1664	2595	− 0.98
7	0.003533	0.000563	0.282067	0.000014	− 22.4	1651	2585	− 0.96
8	0.004534	0.000731	0.282063	0.000018	− 22.5	1664	2595	− 0.98
9	0.004764	0.000653	0.282089	0.000015	− 21.6	1624	2536	− 0.98
10	0.006185	0.000495	0.282070	0.000018	− 22.3	1644	2578	− 0.99
11	0.003542	0.000724	0.282069	0.000017	− 22.3	1655	2581	− 0.98
12	0.002865	0.000834	0.282069	0.000019	− 22.3	1659	2581	− 0.97
13	0.006735	0.000465	0.282087	0.000017	− 21.7	1619	2540	− 0.99
14	0.003096	0.000747	0.282066	0.000015	− 22.4	1660	2587	− 0.98
15	0.005066	0.000750	0.282070	0.000019	− 22.3	1655	2580	− 0.96
16	0.002098	0.000781	0.282089	0.000019	− 21.6	1629	2537	− 0.98
17	0.043665	0.001285	0.282073	0.000016	− 22.2	1674	2574	− 0.96
18	0.055253	0.001508	0.282076	0.000018	− 22.1	1680	2569	− 0.95
19	0.036261	0.001375	0.282064	0.000017	− 22.5	1691	2595	− 0.96

b), comparable Sr–Nb–Pb isotopic composition (Tables 4, 5; Figs. 5, 6), large T_{DM2} model ages (2.8–2.5 Ga; Table 6) and negative ε_{Nd} (t) (from − 19.4 to − 16.8; Table 4) and ε_{Hf} (t) (between − 25.7 and − 21.3; Table 5), implying the ancient enriched and mixed source (crustal and lithospheric mantle). This further supported by their relatively high $Mg^{\#}$ values (27–49; Table 2; Rapp et al. 1999), Ce/Pb average ratios (10.4; Rudnick and Fountain 1995), Nb/Ta ratios (29–58; Table 3; Dostal and Chatterjee 2000), Zr/Hf ratios (32–40; Table 3; Green 1995), and lower Nb/U average ratios (3.53; Table 3; Rudnick and Fountain 1995). Moreover, in the major element versus MgO diagrams (not shown), the studied rocks plot along an extension of the homochronous mafic rocks from Sulu Orogenic Belt trend (Fan et al. 2001; Yang et al. 2005a; Liu 2004; Liu et al. 2005a, b, 2006, 2008a, 2009, 2011, 2012a, b, 2013a, b, c, d, 2014), indicating they were the result of crystal fractionation of a mafic magma similar to the parental magma of the mafic rocks. The studied alkaline rocks thus were products of a mafic magma derived from a mantle source, but with some crustal involvement.

As an important geological process, at present, fractional crystallization has received a certain degree of attention. The studied samples are characterized by higher Rb (125–212 ppm) and Th values (25.2–77.5 ppm; Table 3), $^{207}Pb/^{204}Pb$ (15.381–15.535; Table 5), low Sr/Y

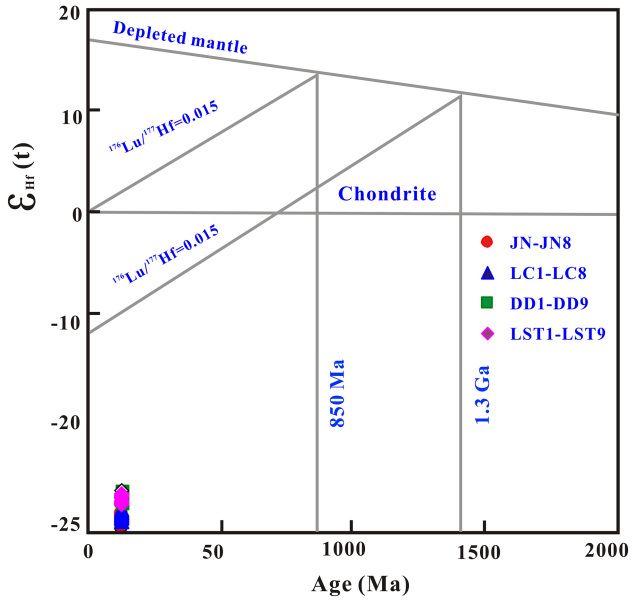

Fig. 7 Plots of zircon ages versus ε_{Hf} (t) values (JN02, LC01, DD02, and LST01) for the alkaline rocks from Sulu Orogenic Belt, eastern NCC

ratios (10.3–21.6; Table 2), implying the fractional crystallization is relatively obvious, on the plots between Ba, Sr, and Eu anomalies (Fig. 10a, b). The parent magma of the studied granites occurred fractionation of potassium feldspar and plagioclase and the plagioclase fractionation is further supported by the Eu negative anomalies (Eu/Eu* = 0.50–0.74) (Fig. 4a). This is also evident in the Ba versus Rb/Sr diagrams (Fig. 11). In general, negative Ti anomalies in all felsic rocks (Fig. 4b) agree with the fractionation of Fe–Ti oxides such as rutile and ilmenite. In contrast, the LC1-LC8 sample experienced a higher degree of separation and crystallization in the genetic process (Fig. 3b, c; Wu et al. 2015).

Assimilation, crystallization fractionation (AFC), or magma mixing is usually postulated to explain the occurrence of felsic rocks (e.g., Depaolo 1981; Marsh 1989). The major and trace element characteristics indicate that crustal contamination is negligible. Generally, for felsic rocks, the AFC process and magma mixing would result in a possible linear correlation between MgO versus ($^{87}Sr/^{86}Sr)_i$ and ε_{Nd} (t) (Fig. 12), these correlations, however, are not observed in the studied alkaline rocks (not shown), indicating that magma evolution is not significantly affected by crustal contamination of magma mixing.

5.2 Genetic mechanism

As discussed above, the alkaline rocks in this study are derived from the partial melting of an ancient and enriched mantle source. A dynamic mechanism, however, is required to decipher the origin of the enriched mantle. Currently, at least three competing mechanisms can be envisaged (Yang et al. 2005a, b; Zhang et al. 2005; Liu et al. 2006, 2008a, 2013c): (1) partial melting of lower-crustal rocks under fluxing of volatile (e.g., Lubala et al. 1994); (2) partial melting of the subducted lithospheric mantle of the Yangtze Craton that has experienced extensive fractionation and minor contamination by crustal material (Yang et al. 2005a); (3) partial melting of the metasomatized mantle, subsequent fractionation of mantle-derived magma with or without crustal contamination (e.g., Sutcliffe et al. 1990; Lynch et al. 1993; Liu et al. 2008a, 2013c). The studied alkaline rocks are characterized by relatively higher ε_{Nd} (t) values than lower-crustal values published for the NCC (Jahn et al. 1999), ruling out the first genetic mechanism for these rocks. At present, it is generally accepted that there is no basic lower crust in eastern China (Gao et al. 1998), however, the first genetic model so far cannot give a reasonable explanation. As discussed above, the studied alkaline rocks were derived from the partial melting of an ancient enriched and mixed source. The parental magma of them thus in this study were derived from the melting of the lithospheric mantle of the NCC, and some ancient continental crust materials were involved during magma ascent by crustal contamination or the source region due to metasomatism. In the Late Mesozoic (160–120 Ma), lithospheric mantle beneath the North China and Yangtze Craton shared similar trace element characteristics, but different Sr–Nd–Pb isotopic ratios (Xie et al. 2006). As discussed above, the Pb isotopic ratios of the studied alkaline rocks from Sulu Orogenic Belt (Table 5) are significantly different from those of the Yangtze lithospheric mantle, and are similar to those of mafic rocks from the central NCC, implying that the studied rocks are not derived from the subducted Yangtze plate, but from the overlying NCC. Therefore, the second genetic model can be eliminated in this study. Owing to its higher density than that of lithospheric mantle peridotite by 0.2–0.4 g cm^{-3}, foundering of lower crustal eclogites into underlying convecting mantle has been proposed to play a role in plume magmatism, crustal evolution and formation of chemical heterogeneities within the mantle (Arndt and Goldstein 1989; Kay and Kay 1991; Rudnick and Fountain 1995; Jull and Kelemen 2001; Escrig et al. 2004; Gao et al. 2004; Elkins-Tanton 2005; Lustrino 2005; Anderson 2006; Gao et al. 2008). This mechanism currently has been reasonably used for explaining the origin of some Mesozoic igneous rocks from the NCC (e.g., Liu et al. 2008a, b, 2009, 2010a, b, 2012a, b, 2013a, b, c, d, 2014, 2015, 2017a, b, 2018). The Pb-isotopic differences observed in the studied rocks from Sulu Belt are not related to the subducted Yangtze lithosphere but result from the contribution

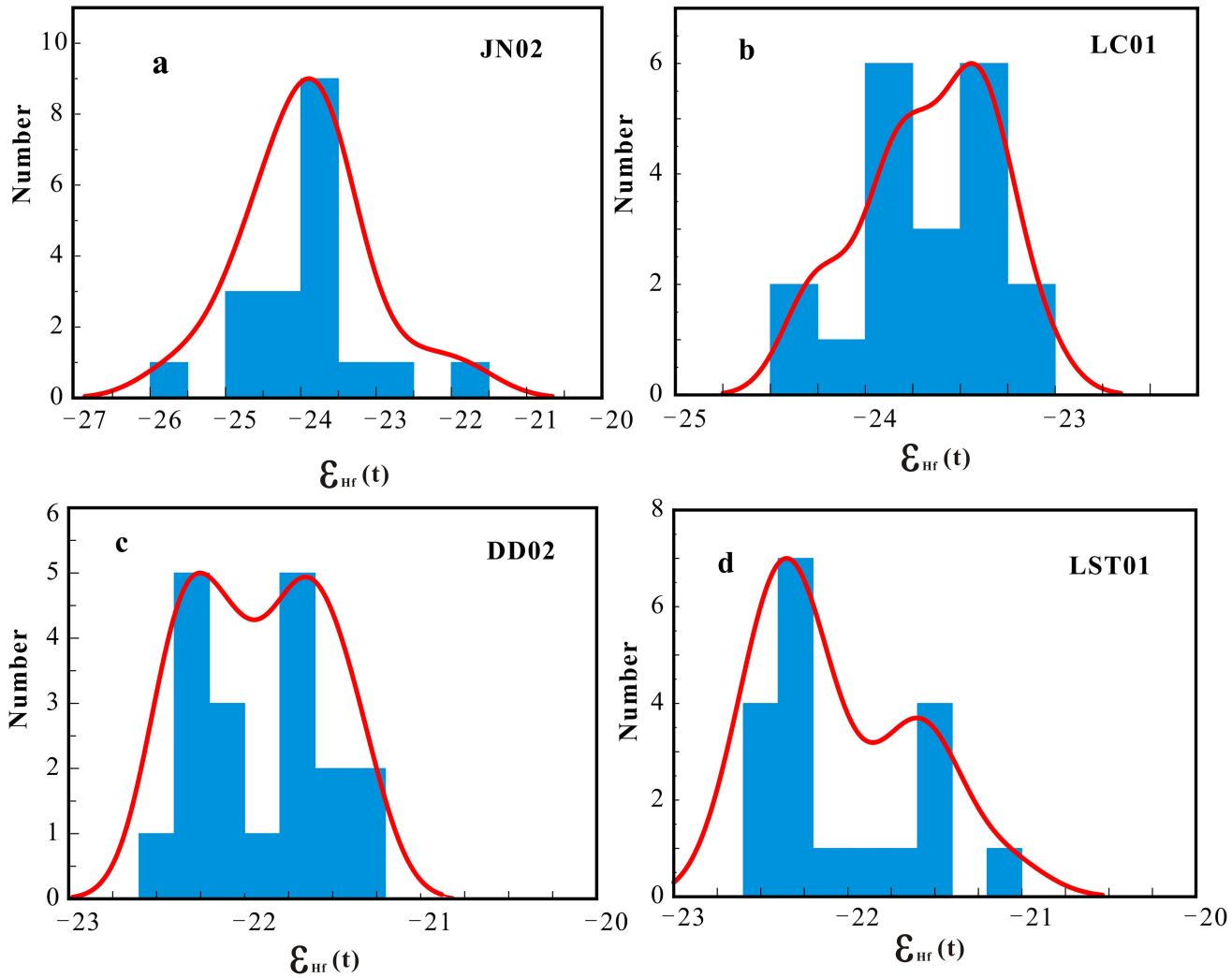

Fig. 8 Histogram of zircon ε_{Hf} (t) values for the alkaline rocks from the Sulu Orogenic Belt, eastern NCC

made by the ascending asthenospheric mantle following Late Mesozoic lithospheric thinning (200–120 Ma; Yang et al. 2004). This also can be used to interpret the origin of the Early Cretaceous mafic rocks from Dabie terrane (Huang et al. 2003). Consequently, we suggest that the Sr, Nd, Pb, and zircon Hf isotopic compositions of the alkaline rocks from central Sulu Orogenic Belt is not due to the involvement of subducted Yangtze lithosphere, but essentially caused by the upwelling of asthenospheric mantle following foundering of lower crustal materials during the Late Triassic (< 200 Ma) and Early Cretaceous (120 Ma; Guo et al. 2004). Nevertheless, the genetic mechanism and process for the studied alkaline rocks must be given a reasonable explanation (Fig. 13).

Nowadays, it is generally believed that between ~ 240 and 220 Ma (Zhang et al. 2005; Yang et al. 2005b; Liu et al. 2008a, b, c, 2009, 2013c), the continual collision between the NCC and Yangtze Craton induced a thickened crust (e.g., Liu et al. 2008a, b, 2009, 2013c), as well as the peak metamorphism and rapid exhumation of the HP–UHP Orogenic terrane (Guo et al. 2006); during ~ 225–205 Ma, the break-off of the subducted Yangtze plate occurred (Chen et al. 2003); between ~ 205 and 185 Ma, further thickened crust appeared due to intracontinental compression between the NCC and Yangtze Craton (e.g., Liu et al. 2008a, b, 2009, 2013c). Subsequently, at ~ 185–165 Ma, asthenospheric upwelling, uplift of Sulu Orogenic Belt, lithospheric collapse, extension and thinning, and emplacement of alkaline magmas occurred beneath the Sulu-Dabie Orogenic Belt and eastern NCC (150–110 Ma; e.g., Li et al. 2002; Liu et al. 2008a, b, 2009, 2013c). And then decompression

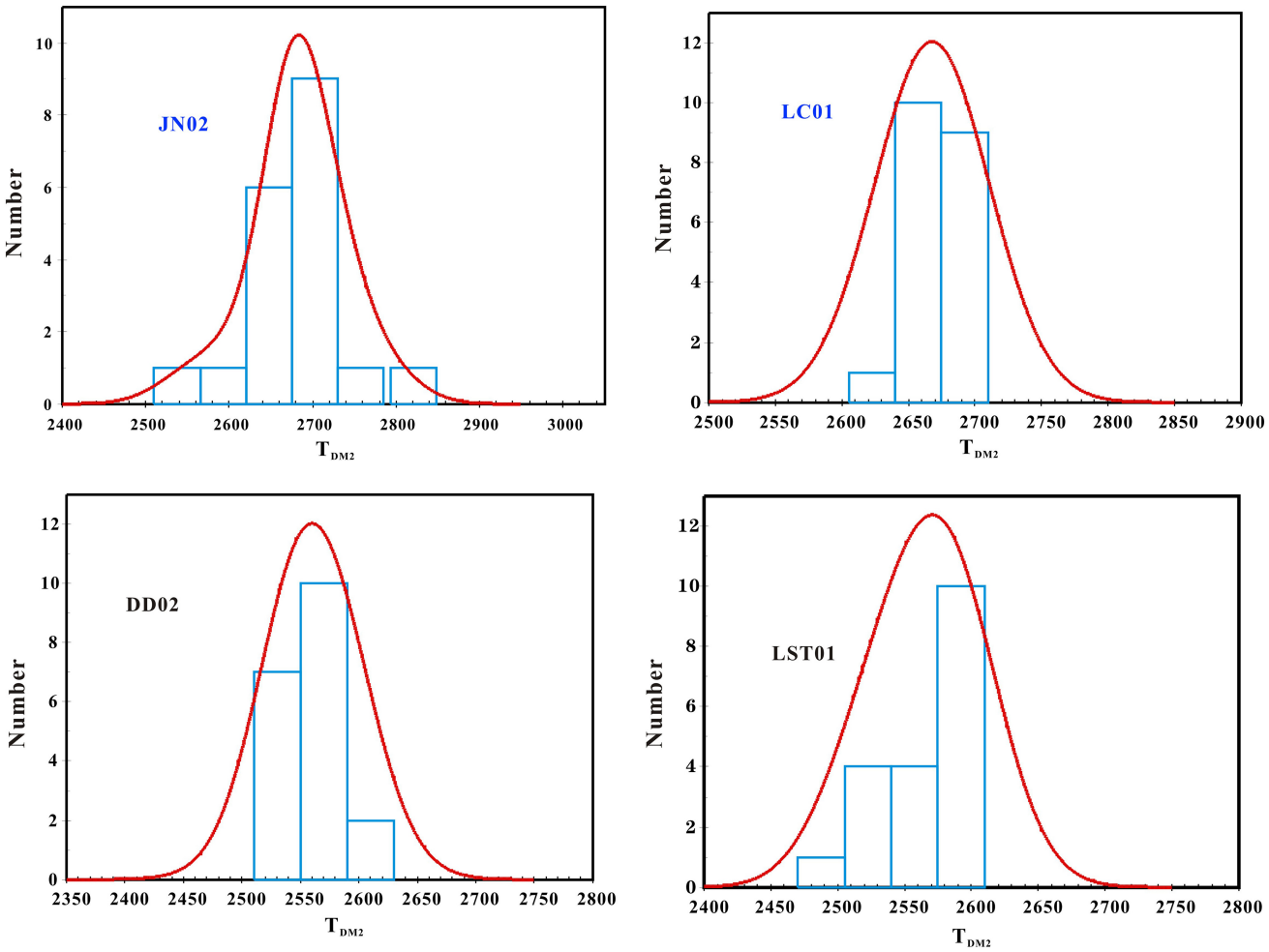

Fig. 9 Histogram of zircon TDM model ages for the alkaline rocks from the Sulu Orogenic Belt, eastern NCC

melting of the thickened crust produced primary melts, which underwent fractionation (i.e., potassium feldspar and plagioclase, rutile and ilmenite) without crustal contamination to produce the alkaline rocks intrusions in the study areas.

6 Tectonic implications

In general, A-type granites occur in the lithospheric extensional setting, and their research has been highly concerned (Liu et al. 2008a; Jiang et al. 2012; Zhang et al. 2020). Previous studies have shown that (Jiang et al. 2012; Zhang et al. 2020), A-type granites can be divided into two types: non-orogenic and post-orogenic (A1 and A2). The A1-type granites were formed in the extension stage after the stability of the continental lithosphere, while the A2-type granites were a sign of the end of orogeny (Eby 1992). The study of A-type granite thus is of great significance in tectonic indication. Currently, it is generally accepted that there exist three stages of magmatism after the UHP metamorphic event (240–220 Ma; Yang et al. 2005b), i.e., Late Triassic, Late Jurassic, and Early Cretaceous. Early Cretaceous magmatic activities (130–110 Ma) were widespread in Sulu Orogenic Belt, petrological, geochronological and geochemical data emphasize that the Early Cretaceous magmatism from the Dabie-Sulu Orogenic Belt has been proposed to result from partial melting of a metasomatized lithospheric mantle source post-collisional extension and thinning after the collision of the NCC and Yangtze Craton (Zhao et al. 1997; Ma et al. 1998; Jahn et al. 1999; Fan et al. 2001; Chen et al. 2001, 2004; Yan et al. 2003, 2005; Li et al. 2004; Yang et al. 2004, 2005a, b; Wang et al. 2005; Huang et al. 2005; Zhang et al. 2005, 2010; Xie et al. 2006; Liu et al. 2006, 2008a, b, 2009; Zhang 2010; Zhao and Zheng 2009; Wang et al. 2009, 2010a, b; Chen and Jiang 2011), displaying features similar to other alkaline rocks referred to in the literature as post-

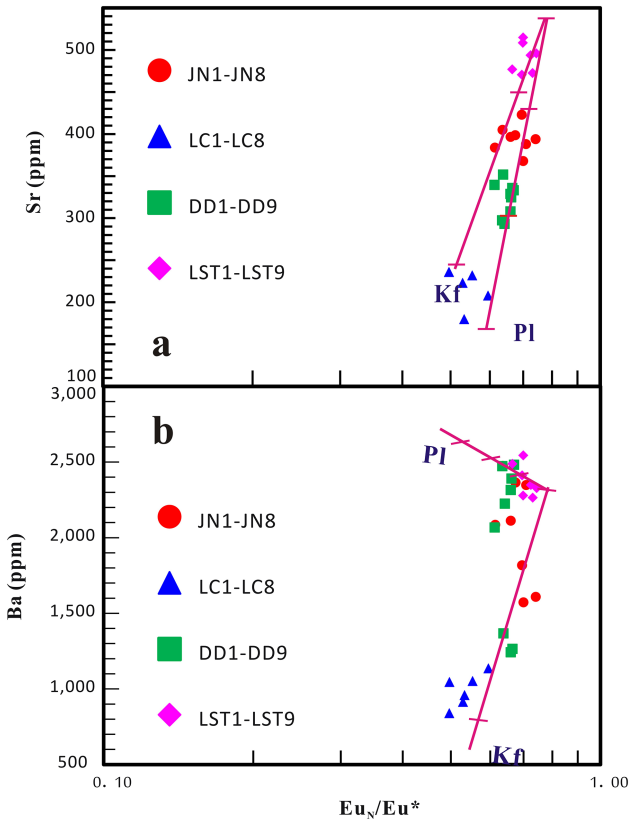

Fig. 10 Plots of **a** Eu_N/Eu^* versus Sr, and **b** Ba for the A-type granites. Mineral fractionation vectors calculated using partition coefficients from Schnetzier and Philpotts (1970). Tick mark indicate percentage of mineral phase removed, in 10% intervals. Pl-plagioclase; Kf-potassium feldspar

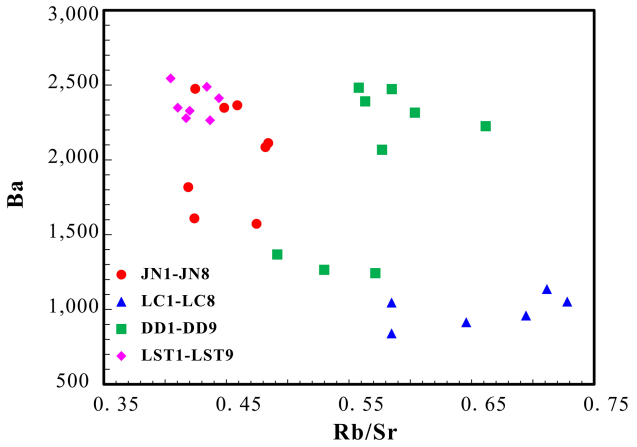

Fig. 11 Plots of Ba versus Rb/Sr for the A-type granites

collisional (Sylvester 1989) or post-orogenic/anorogenic syenites (Bonin 1990). The exact mechanism of lithospheric extension and thinning, however, remains controversial. Firstly, previous studies have shown that all

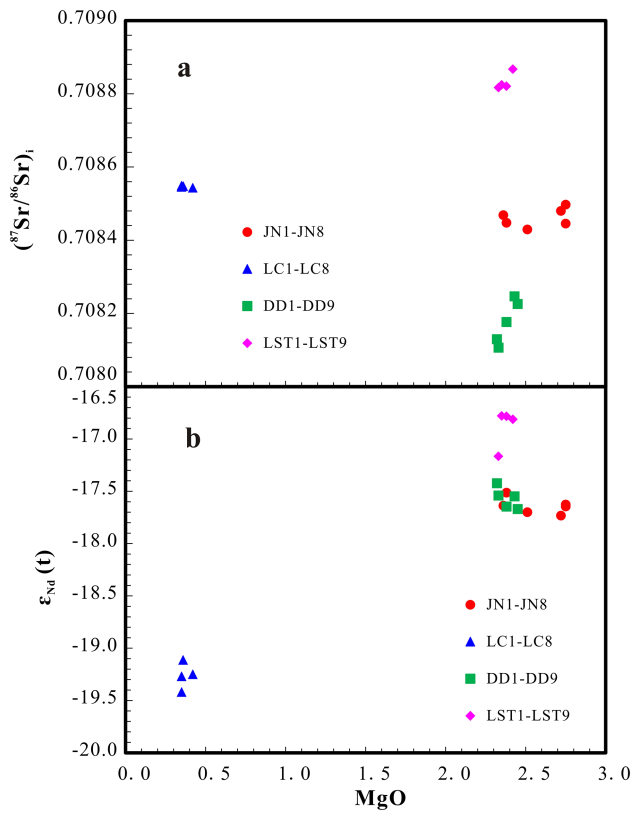

Fig. 12 Plots of MgO versus $(^{87}Sr/^{86}Sr)_i$ and ε_{Nd} (t) for the A-type granites

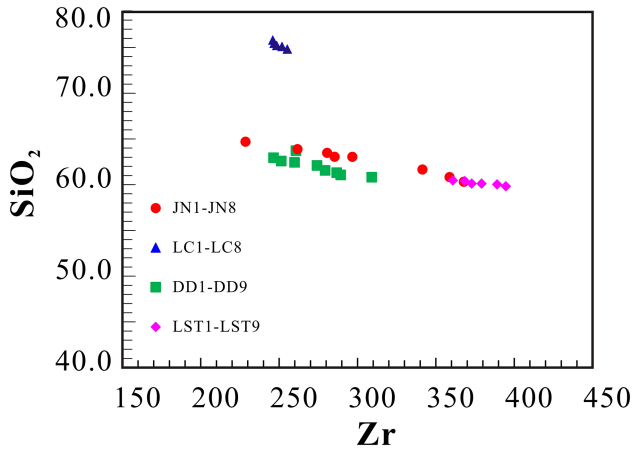

Fig. 13 Plots of Zr versus SiO_2 for the A-type garnites

Mesozoic magmatism in eastern China was the result of a back-arc extensional setting due to the subduction of Izanagi Plate beneath the East Asian continent (Chen et al. 2004). Nevertheless, the Early Cretaceous was a period when the Izanagi Plate primarily moved toward the north or north-northeast, thence, providing little chance for inducing broad back-arc extension in the study areas (Maruyama and Send 1986; Kimura et al. 1990; Li et al.

2004; Liu et al. 2008a). In addition, another model also is recommended (Houseman et al. 1981), i.e., lithospheric extension and thinning have been induced by convective instability of a thickened mantle boundary layer. However, this model has been excluded due to the absence of magmatism (185–165 Ma) in the Sulu Orogenic Belt (Zhao et al. 1997; Fan et al. 2001; Chen et al. 2003; Guo et al. 2004, 2005, 2006; Huang et al. 2005; Yang et al. 2005a, b; Liu et al. 2008a, b, 2009). Currently, lithosphere removal in eastern China has been well recognized and verified (Menzies et al. 1993; Menzies and Xu 1998; Griffin et al. 1998; Wu et al. 2003; Gao et al. 2002), as discussed above, lithospheric foundering can be explained as lithospheric removal, undoubtedly, this model (lithospheric removal) would result in lithospheric extension, thinning and coeval magmatism during Early Cretaceous (130–110 Ma) beneath the Sulu Orogenic Belt (Kay and Kay 1993; Liu et al. 2008a, b, 2009).

7 Conclusions

Several conclusions can be drawn from the petrological and geochemical studies of the studied alkaline rocks:

1. LA-ICP-MS U–Pb zircon dating results indicate that the Jiaonan, Liangcheng, Dadian, and Lanshantou alkaline intruded at 121.3, 123.0, 127.1, and 119.5 Ma, respectively. They are all relatively high in total alkalis ($K_2O + Na_2O$ = 8.32–10.11 wt %); enriched in LREE, LILE (Rb, Th, and U), and Pb and depleted in Nb, Ta, and Ti; and moderate negative Eu anomalies (Eu/Eu* = 0.50–0.74).
2. The alkaline rocks in this study are derived from the partial melting of an ancient and enriched mantle source. The parental magma originated by partial melting of hybridized mantle derived from foundered lower crustal eclogites. Subsequent fractionation of potassium feldspar, plagioclase, Fe–Ti oxides (i.e., rutile, ilmenite). The zircon saturation temperatures (T_{Zr}) of the A-type granites are 830–907 °C, which approximately represents the crystallization temperature of the magma in this study.
3. It is proposed that the occurrence of lithospheric extension and thinning beneath the Sulu Orogenic Belt is related to lithospheric removal due to foundering (removal) of the lower crust.

Acknowledgements This research was supported by the National Natural Science Foundation of China (41373028 and 41573022). The authors thank Honglin Yuan for assistance during zircon Hf isotope analyses and Liang Qi for assistance during Sr–Nd–Pb isotope and trace element analyses, and the zircon U–Pb dating.

References

Altherr R, Holl A, Hegner E (2000) High-potassium, calc-alkaline I-type plutonism in the European Variscides: northern Vosges (France) and northern Schwarzwald (Germany). Lithos 50:51–73

Andersen T (2002) Correction of common lead in U–Pb analyses that do not report 204Pb. Chem Geol 192:59–79

Anderson DA (2006) Speculations on the nature and cause of mantle heterogeneity. Tectonophysics 146:7–22

Arndt NT, Goldsterin SL (1989) An open boundary between lower continental crust and mantle: its role in crust formation and crustal recycling. Tectonophysics 161:201–212

Barry TL, Kent RW (1998) Genozoic magmatism in Mongolia and the origin of central and east Asian basalts. In: Flower MFJ, Chung SL, Lo CH, Lee TY (eds) Mantle dynamics and plate interactions in east Asia. American geophysical union-geodynamics series, vol 27. Wiley, London, pp 347–364

Bonin B (1990) From orogenic to anorogenic settings: evolution of granitoid suite after a major orogenesis. Geol J 25:261–270

Chen JZ, Jiang N (2011) Petrogenesis of the late-Triassic alkaline magmatism in the Jiaodong area: evidence from U–Pb ade, Hf–O isotopes of zircons. Acta Petrol Sin 27:3557–3574 **(in Chinese with English abstract)**

Chen JF, Yan J, Xie Z, Xu X, Xing FM (2001) Nd and Sr isotopic compositions of igneous rocks from the lower Yangtze region in eastern China: constraints on sources. Phys Chem Earth Part A 26:719–731

Chen JF, Xie Z, Li HM, Zhang XD, Zhou TX, Park YS, Ahn KS, Chen DC, Zhang X (2003) U–Pb zircon ages for a collision-related K-rich complex at Shidao in the Sulu ultrahigh pressure terrane, China. Geochem J 37:35–46

Chen B, Jahn BM, Arakawa Y, Zhai MG (2004) Petrogenesis of the Mesozoic intrusive complexes from the southern Taihang Orogen, North China Craton: elemental and Sr–Nd–Pb isotopic constraints. Contrib Mineral Petrol 148:489–501

Chen YB, Mao JW, Spandler C (2013) Petrolgenesis and implications of the Gejiu igneous complex in the western Cathaysia block, south China. Lithos 175–176:213–229

Cheng XJ, Cheng JP, Wang JH (1998) Elemental geochemistry of potassium lamprophyre in Pengjiayu gold deposit, Eastern Shandong. Geochimica 1:91–100 **(in Chinese with English abstract)**

Chung SL, Chu MF, Zhang Y, Xie Y, Lo CH, Lee TY, Lan CY, Li X, Zhang Q, Wang Y (2005) Tibetan tectonic evolution inferred from spatial and temporal variation in post-collisional magmatism. Earth Sci Rev 68:17

Daly RA (1914) Igneous rocks and their origin. McGraw-Hill, New York

Depaolo DJ (1981) Trace element and isotopic effects of combined wallrock assimilation and fractionation crystallization. Earth Planet Sci Lett 53:189–202

Dilek Y, Altunkaynak S (2007) Genozoic crust evolution and mantle dynamics of post-collisional magmatism in Western Anatolia. Int Geol Rev 49:431–453

Ding Y (1989) Study on weak alkaline and alkaline rock petrology in ankang and adjacent areas of Shaanxi province. Master thesis from China University of geosciences (**in Chinese with English abstract**)

Dostal J, Chatterjee AK (2000) Contrasting behaviour of Nb/Hf and ration in a peraluminous granitic pluton (Nova Seotia, Canada). Chem Geol 163:207–218

Eby GN (1992) Chemical subdivision of the A-type granitoids: petrogenesis and tectonic implication. Geology 20:641–644

Elkins-Tanton LT (2005) Continental magmatism caused by lithopheric delamination. In: Foulger GR, Natland JH, Presnall DC,

Anderson DL (Eds.), Plates, Plumes, and Paradigms. Geological Society of London Special Publication 388: 449-462

Escrig S, Capmas F, Dupre B, Allegre GJ (2004) Osmium isotopic constraints on the nature of the DUPAL and anomaly from Indian mid-ocean-ridge basalt. Nature 431:59–63

Fan WM, Guo F, Wang YJ, Lin G, Zhang M (2001) Postorogenic bimodal volcanism along the Sulu orogenic belt in eastern China. Phys Chem Earth (A) 26:733–746

Gao S, Zhang B-R, Jin Z-M, Kern H, Luo T-C, Zhao Z-D (1998) How mafic is the lower continental crust? Earth Planet Sci Lett 106:101–117

Gao S, Rudnick RL, Carlson RW, Mcdonough WF (2002) Re–Os evidence for replacement of ancient mantle lithosphere beneath the North China craton. Earth Planet Sci Lett 198:307–322

Gao S, Rudnick RL, Yuan HL, Liu XM, Liu YS, Xu WL, Ling WL, Ayers JW, Wang XC, Wang QH (2004) Recycling lower continental crust in the North China craton. Nature 432:892–897

Gao S, Rudnick RL, Xu WL, Yuan HL, Liu YS, Walker RJ, Puchtel I, Liu XM, Huang H, Wang XR, Yang J (2008) Recycling deep cratonic lithosphere and generation of intraplat magmatism in the North China Craton. Earth Planet Sci Lett 270:41–53

Green TH (1995) Signifieance of Nb/Ta as an indicator of geochemical processes in the crust mantle system. Chem Geol 120:347–359

Griffin WL, Zhang A, O'Reilly SY, Ryan CG (1998) Phanerozoic evolution of the lithosphere beneath the Sino-Korean Craton. Mantle dynamics and plate interaction in East Asia. In: Flower MF, Chuang SL, Lo CH, Lee TY (eds) Geodynamic series. American Geophysical Union, Washington, D.C, pp 107–126

Griffin WL, Pearson NI, Belousova EA, Saeed A (2006) Comment: Hf-isotope heterogeneity in zircon 91500. Chem Geol 233:358–363

Guo F, Fan WM, Wang YJ, Zhang M (2004) Origin of early Cretaceous calc-alkaline lamprophyres from the Sulu orogen in eastern China: inplicaiton for enrichment processes beneath continertal collisional belt. Lithos 78:291–305

Guo JH, Chen FK, Zhang XM, Siebel W, Zhai MG (2005) Evolution of syn- to post-collisional magmatism from north Sulu UHP belt, eastern Chian: zircon U–Pb geochronology. Acta Petrol Sin 21:1281–1301 **(in Chinese with English abstract)**

Guo F, Fan WM, Li CW (2006) Geochemistry of late Mesozoic adakites from the Sulu belt, eastern China: magma genesis and implications for crustal recycling beneath continental collisional orogens. Geol Mag 143:1–13

Guo Z, Li HQ, Peng H, Feng CX, Chen JJ, Liu S, Guo XL, Feng Q (2016) K–Ar geochronological, geochemical, and Sr–Nd isotopic constraints on the origin of Mafic dykes in the central Tancheng-Lujiang Fault, Shandong Province, China. Bull Mineral Petrol Geochem 35:592–601 **(in Chinese with English abstract)**

Han ZZ (2000) Sulu alkaline rock formation and its tectonic setting. Shandong Geol 16:5–10 **(in Chinese with English abstract)**

Harker A (1896) The natural history of igneous rocks, I. Their geographical and chronological distribution. Sci Prog 6:12–33

Hart SR (1984) A large-scale isotope anomaly in the southern hemisphere mantle. Nature 309:753–757

Hou ML, Jiang YH, Jiang SY, Ling HF, Zhao KD (2007) Contrasting origins of late Mesozoic adakitic grnitoids from the northwestern Jiaodong Peninsula, east China: implications for crustal thickening to delamination. Geol Mag 144:619–631

Houseman GA, McKenzie DP, Moinar P (1981) Convective instability of a thickened boundary laver and its relevance for the thermal evolution of continental convergent belts. J Geophys Res 86:6115–6132

Huang F, Li SG, Zhou HY, Li HM (2003) U–Pb isotopic geochemistry of the post-collisional mafic-ultramafic rocks from the Dabie Mountains-crust-mantle interaction and LOMU component. Sci China 46:320–332

Huang J, Zheng YF, Wu YB, Zhao ZF (2005) Geochemistry of elements and isotopes in igneous rocks from the Wulian region in the Sulu orogen. Acta Petrol Sin 21:545–568 **(in Chinese with English abstract)**

Huang WL, Xu JF, Chen JL, Huang F, Zeng YC, Pi QH, Cai YF, Jiang XZ (2016) Geochronology and geochemistry of the Gejiu complex in the Yunnan province, SW China: petrogenesis and contributions of mantle-derived melts to tin mineralization. Acta Petrol Sin 32:2330–2346 **(in Chinese with English abstract)**

Irvine TN, Baragar RA (1971) A guide to the chemical classification of the common volcanic rocks, Canadian. J. Earth Sci 5:523–548

Jahn BM, Cornichet J, Cong BL, Yui TF (1996) Ultrahigh-εNd eclogites from an ultrahigh-pressure metamorphic terrane of China. Chem Geol 127:61–79

Jahn BM, Wu FY, Lo CH, Tsai CH (1999) Crustmantle interaction induced by deep subduction of the continental crust: geochemical and Sr-Nd isotopic evidence from post-collisional mafic-ultramafic intrusions of the northern Dabie complex, central China. Chem Geol 157:119–146

Jiang B, Gong QJ, Zhang J, Ma N (2012) Late Cretaceous aluminium A-type granites and its geological significance of Dasongpo Sn deposit, Tengchong, West Yunan. Act Prtol Sin 28:1477–1492 **(in Chinese with English abstract)**

Jull M, Kelemen PB (2001) On the conditions for lower crustal convective instability. J Geophys Res 106:6423–6446

Kay RW, Kay SM (1991) Creation and destruction of lower continental crust. Geol Rundsch 80:259–278

Kay RW, Kay SM (1993) Delamination and delamination magmatism. Tectonophysics 219:177–189

Ke S, Luo ZH, Mo XX (2006) Mineralogy of Taxkorgan Cenozoic alkaline complex in Xinjiang and its implication to plution genesis. Acta Petrol Mineral 25:148–156 **(in Chinese with English abstract)**

Kim JN, Han RY, Zhao L, Li QL, Kim SS (2016) Study on the petrographic and SIMS zircon U–Pb geochronological characteristics of the magmatic rocks associated with the Jongju and Cholsan REE deposits in northern Korean Peninsula. Acta Petrol Sin 32:3123–3138 **(in Chinese with English abstract)**

Kimura G, Takahashi M, Kono M (1990) Mesozoic collision extrusion tectonics in eastern Asia. Tectonophysics 181:15–23

Kogarko LN, Kononova VA, Orlova P, Woolley AR (1995) Alkaline rocks and carbonatites of the world (part 2: former USSR). Springer, Netherlands

Le Maitre RW (2002) Igneous rocks: a classification and glossary of terms. Cambridge University Press, Cambridge, p 236

Li S (1991) Age and genesis of the alkaline rocks in northern Hubei province. Acta Petrol Sin 3:27–36 **(in Chinese with English abstract)**

Li XH, Zhou HW, Liu Y, Li JY, Sun M, Chen ZH (1999) The Potassium intrusive rock belt and its petrological and geochemical characteristics, southeast of Guangxi province. Chin Sci Bull 44:1992–1998 **(in Chinese with English abstract)**

Li SG, Huang F, Li H (2002) Post-collisional delamination of the lithosphere beneath Dabie-Sulu orogenic belt. Chin Sci Bull 46:1487–1490

Li XH, Chung SL, Zhou H, Lo CH, Liu Y, Chen CH (2004) Jurassic intraplate magmatism in southern Hunan-eastern Guangxi: 40Ar/39Ar dating, geochrmistry, Sr-Nd isotopes and implications for the tectonic evolution of SE China. In: Malpas J, Fletcher CJN, Ali JR, Aitchison JC (Eds.). aspects of the tectonic evolution of China, Geology Society of London, Special Publication 226: 193-215

Litvinovsky BA, Jahan BM, Zanvilevich AN, Shadaev MG (2002) Crystal fractionation in the petrogenesis of an alkali

monzodiorite-syenite series: the Oshurkovo plutonic sheeted complex, Transbaikalia, Russia. Lithos 64:97–130
Liu S (2004) The Mesozoic magmatism and crustal extension in Shandong Province, China-additionally discussing the relationship between lamprophyres and gold mineralization. Ph.D thesis from Institute of Geochemistry, Chinese Academy of Sciences
Liu S, Hu RZ, Zhao JH, Feng CX (2004a) K–Ar ages of Mesozoic mafic dyke rocks and crustal extension in Shandong Province, eastern China. Acta Geol Sin 78:1207–1213
Liu S, Hu RZ, Zhao JH, Feng CX (2004b) Genesis and source characteristics of the Mafic-Ultramafic Dikes in West Shandong Province: evidence from petrology and geochemistry. Geol Rev 50:577–586 **(in Chinese with English abstract)**
Liu S, Hu RZ, Zhao JH, Feng CX (2005a) Elemental geochemistry and its genesis of Mesozoic dyke in Shandong province. Geochimica 34:339–350 **(in Chinese with English abstract)**
Liu S, Hu RZ, Zhao JH, Feng CX, Zhong H, Cao JJ, Shi DN (2005b) Chemical characteritics and petrogenic investigation of the Late Mesozoic lamprophyres of Jiaobei, Shandong province. Acta Petrol Sin 21:947–958 **(in Chinese with English abstract)**
Liu S, Zou HB, Hu RZ, Zhao JH, Feng CX (2006) Mesozoic mafic dikes from the Shandong Peninsula, North China Craton: petrogenesis and tectonic implications. Geochem J 40:181–195
Liu S, Hu RZ, Gao S, Feng CX, Qi L, Zhong H, Xiao TF, Qi YQ, Wang T, Coulson IM (2008a) Zircon U–Pb geochronology and major, trace elemental and Sr–Nd–Pb isotopic geochemistry of mafic dykes in western Shandong Province, east China: constrains on their petrogenesis and geodynamic significance. Chem Geol 255:329–345
Liu S, Hu RZ, Gao S, Feng CX, Qi YQ, Wang T, Feng GY, Coulson IM (2008b) U–Pb zircon age, geochemical and Sr–Nd–Pb–Hf isotopic constraints on age and origin of alkaline intrusions and associated mafic dikes from Sulu orogenic belt, eastern China. Lithos 106:365–379
Liu S, Hu RZ, Gao S, Feng CX, Yu BB, Qi YQ, Wang T, Feng GY, Coulson IM (2008c) Zircon U–Pb age, geochemistry and Sr–Nd–Pb isotopic compassion of adakitic volcanic rocks from Joaodng, Shandong province, eastern Chain: constraints on petrogenesis and implications. J Asian Earth Sci 35:445–458
Liu S, Hu RZ, Gao S, Feng CX, Yu BB, Feng GY, Qi YQ, Wang T, Coulson IM (2009) Petrogenesis of late Meosozic mafic dykes in the Jiaodong peninsula, eastern North China Craton and implications for the foundering of lower crust. Lithos 113:621–639
Liu S, Hu RZ, Feng GY, Yang YH, Feng CX, Qi YQ, Wang T (2010a) Distribution and significance of the mafic dyke swarms since Mesozoic in the North China Craton. Geol Bull China 29:259–267 **(in Chinese with English abstract)**
Liu S, Hu RZ, Gao S, Feng CX, Feng GY, Coulson IM, Li C, Wang T, Qi YQ (2010b) Zircon U–Pb age and Sr–Nd–Hf isotope geochemistry of Permian granodiorite and associated gabbro in the Songliao Block, NE China and implications for growth of juvenile crust. Lithos 114:423–436
Liu YS, Hu ZC, Zong KQ, Gao CG, Gao S, Xu J, Chen HH (2010c) Reappraisement and refinement of zircon U–Pb isotope and trace element analyses by LA-ICP-MS. Chin Sci Bull 55:1535–1546
Liu S, Hu RZ, Gao S, Feng CX, Zhong H, Wang T, Feng GY, Yang YH (2011) U–Pb zircon age along with geochemical and Sr-Nd-Pb isotopic constraints on the dating and origin of intrusive complexes from the Sulu orogenic belt, Eastern China. Int Geol Rev 53:61–83
Liu S, Hu RZ, Gao S, Feng CX, Feng GY, Qi YQ, Coulson IM, Yang YH, Yang CG, Tang L (2012a) Geochemical and isotopic constraints on the age and origin of mafic dikes from Eastern Shandong province, Eastern North China Craton, China. Int Geol Rev 54:1389–1400
Liu S, Hu RZ, Gao S, Feng CX, Coulson IM, Feng GY, Qi YQ, Yang YH, Yang CG, Tang L (2012b) U–Pb zircon age, geochemical and Sr-Nd isotopic data as constraints on the petrogenesis and emplacement time of the Precambrian mafic dyke swarms in the North China Craton (NCC). Lithos 140–141:38–52
Liu S, Feng CX, Hu RZ, Gao S, Wang T, Feng GY, Qi YQ, Coulson IM, Lai SC (2013a) Zircon U–Pb age, geochemical, and Sr–Nd–Pb isotopic constraints on the origin of alkaline intrusions in eastern Shandong province, China. Miner Petrol 107:591–608
Liu S, Feng CX, Jahn B, Hu RZ, Gao S, Coulson IM, Feng GY, Lai SC, Yang CG, Yang YH (2013b) Zircon U–Pb age, geochemical, and Sr–Nd–Hf isotopic constraints on the origin of mafic dykes in the Shaanxi Province, North China Craton, China. Lithos 175–176:244–254
Liu S, Hu RZ, Feng CX, Gao S, Feng GY, Lai SC, Qi YQ, Coulson IM, Yang YH, Yang CG, Tang L (2013c) U–Pb zircon age, geochemical, and Sr–Nd–Pb isotopic constraints on the age and origin of mafic dykes from eastern Shandong Province, eastern China. Acta Geol Sin 87:1045–1057
Liu S, Hu RZ, Gao S, Feng CX, Coulson IM, Feng GY, Qi YQ, Yang YH, Yang CG, Tang L (2013d) Zircon U–Pb age and Sr–Nd–Hf isotopic constraints on the age and origin of Triassic mafic dikes, Dalian area, Northeast China. Int Geol Rev 55:249–262
Liu S, Feng CX, Jahn BM, Hu RZ, Zhai MG, Lai SC (2014) Zircon U–Pb age, geochemical, and Sr–Nd isotopic constraints on the origin of late Carboniferous mafic dykes of the north China Craton, Shanxi province, China. Acta Petrol Sin 30:1707–1717
Liu S, Feng CX, Hu RZ, Zhai MG, Gao S, Lai SC, Yan J, Coulson IM, Zou HB (2015) Zircon U–Pb geochronological, geochemical, and Sr–Nd isotope data for early Cretaceous mafic dykes in the Tancheng-Lujiang Fault area of the Shandong province, China: constraints on the timing of magmatism and magma genesis. J Asian Earth Sci 98:247–260
Liu S, Feng CX, Zhai MG, Hu RZ, Lai SC, Chen JJ, Yan J (2016) Zircon U–Pb age, geochemical, and Sr-Nd-Hf isotopic constraints on the origin of early Cretaceous mafic dykes from western Shandong province, eastern North China Craton. Acta Petrol Sin 32:629–645
Liu S, Feng CX, Feng GY, Xu MJ, Guo XL, Feng Q, Yan J, Guo Z (2017a) Zircon U–Pb age, geochemical and Sr–Nd–Pb isotopic data: constraints on the genetic model of the mafic dykes from the North China Craton. Acta Petrol Sin 33:1667–1685
Liu S, Feng CX, Feng GY, Xu MJ, Coulson IM, Guo XL, Guo Z, Peng H, Feng Q (2017b) Timing, mantle source and origin of mafic dykes within the gravity anomaly belt of the Taihang-Da Hinggan gravity lineament, central North China Craton. J Geodyn 109:41–58
Liu S, Feng CX, Santosh M, Feng GY, Coulson IM, Xu MJ, Guo Z, Guo XL, Peng H, Feng Q (2018) Integrated elemental Sr–Nd–Pb–Hf isotopic studies of Mesozoic mafic dykes from the eastern North China Craton: implications for the dramatic transformation of lithospheric mantle. J Geodyn 114:19–40
Lubala RT, Frick C, Roders JH, Walraven F (1994) Petrogenesis of syenites and granites of the Schiel alkaline complex, northern Transvaal, south Africa. J Geol 102:307–309
Lugmair GW, Harti K (1978) Lunar intial 143Nd/144Nd: differential evolution of the lunar crust and mantle. Earth Planet Sci Lett 39:349–357
Lustrino M (2005) How the delamination and detachment of lower crust can influence basaltic magmatism. Earth Sci Rev 72:21–38
Lynch DJ, Musselman TE, Gutmann JT, Patchett PJ (1993) Isotopic evidence for the origin of Cenozoic volcanic rocks in the Pinacate volcanic field, northwestern Mexico. Lithos 29:295–302
Ma CQ, Li Z, Ehlers C, Yang K, Wang R (1998) A post-collisional magmatic plumbing system: Mesozoic granitoid plutons from

the Dabieshan high-pressure and ultrahigh-pressure metamorphic zone, east-central China. Lithos 45:431–456
Marsh JS (1989) Geochemical constraints on coupled assimilation and fractional crystallization involving upper crustal compositions and continental tholeiitic magma. Earth Planet Sci Lett 92:78–80
Maruyama S, Send T (1986) Orogeny and relative plate motions: example of the Japanese Islands. Tectonophysics 127:305–329
Meng FC, Xue HM, Li TF, Yang HR, Liu FL (2005) Enriched characteristics of late Mesozoic manle under the Sulu orogenic belt: geochemical evidence from gabbro in Rushan. Acta Petrol Sin 21:1583–1592 **(in Chinese with English abstract)**
Menzies MA, Xu YG (1998) Geodynamics of the North China Craton. In: Mantle Dynamics and Plate Interactions in East Asia (Flower M.F.J., Chung S.L., Lo C.H., Lee T.Y.), American Geophysical Union, Geodynamics Series 27: 155-165
Menzies MF, Fan WM, Zhang M (1993) Paleozoic and Cenozoic lithosprobes and loss of > 120 km or Archean lithosphere, Sino-Koran Craton, China, magmatic processes and plate tectonic, geological society of London special publication. Academic Press, London
Menzies M, Xu YG, Zhang HF, Fan WM (2007) Integration of geology, geophysics and geochemistry: a key to understanding the North China Craton. Lithos 96:1–21
Middlemost EAK (1972) A simple classification of volcanic rocks. Bull Volconol 36:382–397
Middlemost EAK (1994) Naming materials in the magma/igneous roc system. Earth Sci Rev 74:193–227
Mingram B, Trumbull RB, Littman S, Gerstenberger H (2000) A petrogenetic study of anorogenic felsic magmatism in the Cretaceous Paresis ring complex, Namibia: evidence for mixing of crust and mantle-derived components. Lithos 54:1–22
Potts PJ, Kane JS (2005) International association of geoanalysts certificate of analysis: certified reference material OU-6 (Penrhyn slate). Geostand Geoanal Res 29:233–236
Qi L, Hu J, Grégoire DC (2000) Determination of trace elements in granites by inductively coupled plasma mass spectrometry. Talanta 51:507–513
Qiu JX (1993) Qinba alkaline rock. Geological Publishing House, Beijing **(in Chinese with English abstract)**
Rapp RP, Shimizu N, Norman MD, Applegate GS (1999) Reaction between slab-derived melts and peridotite in the mantle wedge: experimental constraints at 3.8 GPa. Chem Geol 160:335–356
Ren KX, Yan GG, Mu BL, Cai JH, Li FT, Shao HX, Chu ZY (2004) Geochemical characteristics and geological implications of the Hekanzi alkaline complex in Lingyuan County, western Liaoning province. Acta Petrol Mineral 23:193–202
Rudnick RL, Fountain DM (1995) Nature and composition of the continental crust: a lower crustal perspective. Rev Geophys 33:267–309
Schnetzier CC, Philpotts JA (1970) Partition coefficients of rare-earth elements between igneous matrix material and rock-forming mineral phenocrysts: II. Geochim Cosmochim Acta 34:331–340
Shandong Province Geology and Mineral Resources Bureau (1991) Shandong province regional geology. Geological Press, Beijing **(in Chinese with English abstract)**
Shao JA, Zhang YB, Zhang LQ, Mu BL, Wang PY, Guo F (2003) Early Mesozoic dike swarms of carbonatites and lamprophyres in datong area. Acta Petrol Sin 19:93–104 **(in Chinese with English abstract)**
Shao JA, Zhai MG, Zhang LQ, Li DM (2005) Identification of 5 time-groups of Dike Swarms in Shanxi-Hebei-Inner Mongulia Border area and its tectonic implications. Acta Geol Sin 79:56–67 **(in Chinese with English abstract)**
Steiger RH, Jager E (1977) Subcommission on geochronology: convention on the use of decay constants in geochronology and cosmochronology. Earth Planet Sci Lett 36:359–362
Sun SS, McDonough WF (1989) Chemical and isotopic systematics of oceanic basalts: implications for mantle composition and processes. In: Saunders AD, Norry MJ (eds) Magmatism in the ocean basins. Geological Society Special Publication, London, pp 313–345
Sutcliffe EH, Smith AR, Doherty W, Barnett RL (1990) Mantel derivation of Archean amphibole-bearing granitoids and associated mafic rocks: evidence from the southern Superior province, Canada. Contrib Miner Petrol 105:255–274
Sylvester PJ (1989) Post-collional alkaline granites. J Geol 97:261–280
Tan LK (1997). Petrochemistry of several alkaline rock masses in Yinshan area. Master thesis, Peking University (in Chinese with English abstract)
Tang L, Liu S, Feng CX, Feng GY, Yang YH, Qi YQ (2014) Zircon U–Pb geochronology, geochemical compositions of the Mafic dykes from Yangshugou, northern Hebei Province: constraints on the age and petrogenesis. Bull Mineral Petrol Geochem 33:82–90 **(in Chinese with English abstract)**
Thiompson M, Potts PJ, Kane JS, Wilson S (2000) An international proficiency test for analytical geochemistry laboratories-report on round 5 (August 1999). Geostand Geoanal Res 24:E1–E28
Wang Q, Zhen ZH, Xiong XL (2000) The ascertainment of late Yanshanian A-type granitein Tongbai-Dabie Orogenic Belt. Acta Petrol Mineral 19:297–315 **(in Chinese with English abstract)**
Wang YM, Gao YS, Han HM, Wang XH (2003) Practical handbook of reference materials for geoanalysis. Geological Publishing House, Bath **(in Chinese)**
Wang YJ, Fan WM, Peng TP, Zhang HF, Guo F (2005) Nature of the Mesozoic lithospheric mantle and tectonic decoupling beneath the Dabie orogen, central China: evidence from $^{40}Ar/^{39}Ar$ geochronology, elemental and Sr–Nd–Pb isotopic compositions of early Cretaceous mafic igneous rocks. Chem Geol 220:165–189
Wang T, Liu S, Hu RZ, Feng CX, Qi YQ, Feng GY, Wang CH (2009) Elemental geochemistry and petrogenesis of A-type granites in the Sulu Orogenic Belt. J Jilin Univ 39:676–688 **(in Chinese with English abstract)**
Wang Q, Liu S, Hu RZ, Feng CX, Qi YQ, Feng GY, Yang YH (2010a) Petrogenesis of alkaline rocks in the Sulu Orogen: evidence from elemental geochemistry. Acta Mineral Sin 30:194–206 **(in Chinese with English abstract)**
Wang T, Liu S, Hu RZ, Feng CX, Qi YQ, Feng GY, Yang YH (2010b) Petrogenesis of alkaline rocks in the Sulu Orogenic Belt-evidence from elemental geochemistry. Acta Mineral Sin 30:194–206 **(in Chinese with English abstract)**
Wang T, Liu S, Zhou JX, Li YB (2013) Petrogenesis of adamellites from eastern Shandong province: geochronological, geochemical, and Sr–Nd isotopic evidence. Int Geol Rev 55:1786–1800
Whalen JB, Currie KL, Chappell BW (1987) A-type granites: geochemical characteristics, discrimination and petrogenesis. Contrib Miner Petrol 85:801–813
Wilde SA, Zhou XH, Nemchin AA, Sun M (2004) Mesozoic crust-mantle interaction beneath the North China craton: a consequence of the dispersal of Gondwanaland and accretion of Asia. Geology 31:817–820
Wright JB (1969) A simple alkalinity ratio and its application to questions of non-orogenic genesis. Geol Mag 101:370–384
Wu LR (1966) Studies on alkaline rocks in several areas. Science Press, Beijing **(in Chinese with English abstract)**

Wu FY, Xu YG, Gao S, Zheng JP (1998) Lithospheric thinning and destruction of the North China Craton. Acta Petrol Sin 6:1145–1174 **(in Chinese with English abstract)**

Wu FY, Sun DY, Li HM, Jahn BM, Wilde S (2002) A-type granites in northeastern China: age and geochemical constraints on their petrogenesis. Chem Geol 187:143–173

Wu FY, Walker RJ, Ren XW, Sun DY, Zhou XH (2003) Osmium isotopic constraints on the age of lithospheric mantle beneath northeastern China. Chem Geol 197:107–129

Wu FY, Lin JQ, Wilde SA, Zhang X, Yang JH (2005a) Nature and significance of the Early Cretaceous giant igneous event in eastern China. Earth Planet Sci Lett 233:103–119

Wu FY, Yang JH, Wilde SA, Zhang XO (2005b) Geochronology, petrogenesis and tectonic implications of Jurassic granites in the Liaodong Peninsula, NE China. Chem Geol 221:127–156

Wu FY, Walker RJ, Yang YH, Yuan HL, Yang JH (2006) The chemical-temporal evolution of lithospheric mantle underlying the North China Craton. Geochim Cosmochim Acta 70:5013–5034

Wu HJ, He YS, Hou ZH, Li SG (2015) Plagioclase composition of Early Cretaceous granitoid in Dabieshan: fractional crystallization to whole rock: The influence of Sr–Cao relationship. Chin Sci Bull 60:198–205 **(in Chinese)**

Xie YW, Zhang YQ, Zhong SL, Li XH (1999) Trace element characteristics of the Cenozoic high-K alkaline magmatic rock series in the eastern Erhai, Yunnan province. Acta Petrol Sin 15:75–82 **(in Chinese with English abstract)**

Xie Z, Li Q, Gao T et al (2006) Comment on "Petrogenesis of postorogenic syenites in the Sulu Orogenic bet, east China: geochronological, geochemical and Nd–Sr isotopic evidence" by Yang et al. Chem Geol 235:191–194

Xu BL, Yan GH, Mu BL, Tan LP, He ZP, Qiao GS, Zhang QY (1998a) Age of alkaline syropicite and its significance in Liangtun-Gaodonggou, Gai County, Liaoning Province. Chin Sci Bull 43:1885–1887 **(in Chinese with English abstract)**

Xu YG, Menzies MA, Vroon P (1998b) Texture-temperature-geochemistry relationship in the upper mantle as revealed from spine1 peridotite xenoliths from Wangqing, NE China. J Petrol 39:469–493

Xu XY, Cai ZH, Xu ZQ, Cao H (2017) The Miocene High K alkaline rocks in Tashkorgan Region, Northeastern Pamir: formation mechanism and tectonic implications. Geol Rev 63:616–629 **(in Chinese with English abstract)**

Yan GH, Mu BL, Xu BL, He GQ, Tan LK, Zhao H, He ZP, Qiao GS (2000) The characteristics and significance of Sr, Nd and Pb isotopes in alkaline intrusive rocks of Yanliao-Yin-shan Triassic. Sci China 30:383–387 **(in Chinese with English abstract)**

Yan GH, Mu BL, Xu BL (2002) The age, Nd–Pb–Sr isotope and significance of the phaneorozoic alkali-enriched intrusive rock, north China. Geol Rev 48:69–76 **(in Chinese with English abstract)**

Yan J, Chen JF, Yu G, Qian H, Zhou TX (2003) Pb isotopic characteristics of late Mesoozic mafic rocks from the laower Yangtze region: evidence for enriched mantle. J China Univ Geosci 9:195–206 **(in Chinese with English abstract)**

Yan J, Chen J-F, Xie Z, Yang G, Yu G, Qian H (2005) Geochemistry of late Mesozsoic basalts from Kedoushan in the middle and lower Yangtze regions: constraints on characteristics and evolution of the lithospheric mantle. Geochimica 34:455–469 **(in Chinese with English abstract)**

Yan GH, Mu BL, Zeng YS, Cai JH, Ren KX, Li FT (2007) Temporal and spatial distribution and strontium isotope characteristics of the carbonate Rocks from the North China Craton and their geological significance. Geol J China Univ 13:463–473 **(in Chinese with English abstract)**

Yang JH, Chung SL, Zhai MG, Zhou XH (2004) Geochemical and Sr–Nd–Pb isotopic compositions of mafic dikes from the Jiaodong Peninsula, China: evidence for vein-plus-peridotite melting in the lithospheric mantle. Lithos 73:145–160

Yang JH, Chung SL, Wilde SA, Wu FY, Chu MF, Lo CH, Fan HR (2005a) Petrogenesis of post-orogenic syenites in the Sulu Orognic Belt, east China: geochronological, geochemical and Nd–Sr isotopic evidence. Chem Geol 214:99–125

Yang JH, Wu FY, Chung SL, Wilde SA, Chu MF, Lo CH, Song B (2005b) Petrogenesis of early Cretaceous intrusions in the Sulu ultrahigh-pressure orogenic belt, east China and theri relationship to lithospheric thinning. Chem Geol 222:200–231

Yang JH, Wu FY, Shao JA, Wilde SA, Xie LW, Liu XM (2006) Constraints on the timing of uplift of the Yanshan Fold and Thrust Belt, North China. Earth Planet Sci Lett 246:336–352

Yang YH, Liu S, Hu RZ, Feng CX, Feng GY, Yang CG, Qi YQ (2012) Geochemirsty and petrogenesis of the Sanchakou mafic dyke in Chengde, Hebei province. J Jilin Univ 42:1796–1805 **(in Chinese with English abstract)**

Yang CG, Liu S, Feng CX, Feng GY, Yang YH, Qi YQ, Tang L (2013a) Geochemical characteristics and petrogenesis of Mesozoic lamprophyres from Zhangjiahe, South Qinling, China. Acta Minral Sin 1:119–128 **(in Chinese with English abstract)**

Yang YH, Liu S, Hu RZ, Feng CX, Feng GY, Qi YQ, Yang CG, Tang L (2013b) Geochemical features and petrogenesis of Houcheng mafic dyke in Hebei: evidence from jajor and trace elements. Geol Bull China 32:607–616 **(in Chinese with English abstract)**

Ye K, Hirajima T, Ishiwateri A (1996a) Significance of interstitial coesite in eclogites from Yankou, Qingdao city, eastern China. China Sci Bull 41:1047–1048

Ye K, Hirajima T, Ishiwateri A (1996b) Significance of interstitial coesite in eclogites from Yankou, Qingdao city, eastern China. Chin Sci Bull 41:1047–1048 **(in Chinese)**

Ye K, Ye DN, Cong BL (2000) The possible subduction of continental material to depths graster than 200 km. Nature 407:734–736

Yin A, Ni S (1993) An indentation model for the north and south China collision and the development of the Tan-Lu and Honam fault systems, eastern Asia. Tectonics 124:801–813

Ying JF, Zhou XH, Zhang HF (2004) Geochemical and isotopic investigation of the Laiwu-zibo carbonatites from western Shandong Province, China and implications for their petrogenesis and enriched mantle source. Lithos 75:413–426

Yu XF, Tang HS, Han ZZ, Li CY (2010) Geological characteristics and origin of rare earth deposits related with alkaline Rockin Chishan-Longbaoshan Area in Shandong Province. Acta Geol Sin 84:407–417 **(in Chinese with English abstract)**

Zhai MG, Cong BL, Guo JH, Liu WJ, Li YG, Wang Q (2000) Division of petrological-tectonic units in the northern Sulu ultrahigh-pressure zone: an example of thick-skin thrust of crystalline units. Acta Geol Sin 35:16–26 **(in Chinese with English abstract)**

Zhai MG, Fan QC, Zhang HF, Sun J, Shao JA (2007) Lower crustal processes leading to Mesozoic lithospheric thinning beneath eastern North China: Underplating, replacement and delamination. Lithos 96:36–54

Zhang HF (2001) Petrogeochemistry and tectonic significance of alkaline rock zone in indosinian period at the edge of Taipei, north China. Master thesis from Peking University (in Chinese with English abstract)

Zhang J (2010) A geochemical study of Mesozoic magmatic rocks in the Sulu orogen. Ph.D. thesis from University of Science and Technology of China (in Chinese with English abstract)

Zhang HF, Sun M (2002) Geochemistry of Mesozoic basalts and mafic dikes, southeastern north China Carton, and tectonic implications. Int Geol Rev 44:370–382

Zhang YQ, Xie YW (1997) Geochronology and Nd–Sr isotopic characteristics of alkali-rich intrusive rocks in Ailaoshan-Jinsha River. Sci China 27:289–293 **(in Chiese with English abstract)**

Zhang T, Zhang YQ (2007) Geochronological sequence of Mesozoic intrusive magmatism in Jiaodong Peninsula and Its Tectonic Constraints. Geol J China Univ 13:323–336 **(in Chinese with English abstract)**

Zhang HF, Sun M, Lu FX, Zhou XH, Zhou M, Liu YS, Zhang GH (2001) Geochemical significance of a garnet Iherzolite from the Dahongshan kimberlite, Yangtze Craton, southern China. Geochem J 35:315–331

Zhang CL, Gao S, Zhang GW, Liu XM, Yu ZP (2002) Geochemistry and geological significance of alkaline rock wall group in early Paleozoic in southern Qinling. Sci China 32:819–928 **(in Chinese with English abstract)**

Zhang HF, Sun M, Zhou XH, Zhou MF, Fan WM, Zheng JP (2003) Secular evolution of the lithosphere beneath the eastern North China Craton: evidence from Mesozoic basalt and high-Mg andesites. Geochem Cosmochim Acta 67:4373–4387

Zhang HF, Sun M, Zhou MF, Fan WM, Zhou XH, Zhai MG (2004) Highly heterogeneous late Mesozoic lithospheric mantle beneath the North China Craton: evidence from Sr–Nd–Pb isotopic systematics of mafic ifneous rocks. Geol Mag 141:55–62

Zhang HF, Sun M, Zhou XH, Ying JF (2005) Geochemical constraints on the origin of Mesozoic alkaline intrusive complexes from the North China Craton and tectonic implications. Lithos 81:297–317

Zhang HF, Ying JF, Shimoda G, Kita NT, Norishita YH, Shao JA, Tang YJ (2007) Importance of melt circulation and crust-mantle interaction in the lithospheric evolution beneath the North China Craton: evidence from Mesozoic basalt-borne clinopyroxene xenocrysts and pyroxenite xenoliths. Lithos 96:67–89

Zhang J, Zhao ZF, Zheng YF, Dai MN (2010) Postcollisional magmatism: geochemical constraints on the petrogenesis of Mesozoic granitoids in the Sulu orogen. Lithos 119:512–536

Zhang J, Tian H, Li HK, Su WB, Zhou HY, Xiang ZQ, Geng JZ, Yang LG (2015) Age, geochemistry and zircon Hf isotope of the alkaline basaltic rocks in the middle section of the Yan-Liao aulacogen along the northern margin of the North China Craton: new evidence for the brakup of the Columbia supercontinent. Acta Petrol Sin 31:3129–3146 **(in Chinese with English abstract)**

Zhang C, Wu XW, Liu YJ, Zhang YJ, Zhang C, Guo W, Cui FH (2020) Genesis of early Permian A-type granites in the middle of the great Xing'an Range and constraints on tectonic evolution of the Zhailantun area. Acta Petrologica Sinca 36:1091–1106 **(in Chinese with English abstract)**

Zhao ZF, Zheng YF (2009) Subduction of continental lithosphere remelting: the genesis of Mesozoic magmatic rocks in the Dabie-Sulu orogenic belt. Sci China 30:888–909 **(in Chinese with English abstract)**

Zhao G, Wang D, Cao Q (1997) Geochmical features and petrogenesis of Laoshan granite in east Shandong province. Geol J China Univ 3:1–15 **(in Chinese with English abstract)**

Zhen XS, Bian TT (1996) On the Cenozoic volcanic rocks in Hoh Xil district, Qinghai province. Acta Petrol Sin 12:530–545 **(in Chinese with English abstract)**

Zheng YF, Wang ZR, Li SG, Zhao ZF (2002) Oxygen isotope equilibrium between eclogite minerals and its constraints on mineral Sm–Nd chronometer. Geochim Cosmochim Acta 66:625–634

Zheng JP, Griffin WL, O'Reilly SY (2006) Mineral chemistry of garnet peridotites from Paleozoic, Mesozoic and Cenozoic Lithosphere: constraints on mantle evolution beneath Eastern China. J Petrol 47:2233–2256

Zheng JP, Griffin WL, O'Reilly SY, Yu CM, Zhang HF, Prarson N, Zhang M (2007) Mechanism and timing of lithospheric modification and replacement beneath the astern North China Craton: peridotitic xenoliths from the 100 Ma Fuxin basalts and a regional synthesis. Geochim Cosmochim Acta 71:5203–5225

Zhou TH, Lu GX (2000) Tectonics, granitoids and Mesozoic gold deposits in east Shandong, China. Ore Geol Rev 16:71–90

Zhou TX, Chen JF, Zhang X, Li XM (1995) Geochemistry of the North Huaiyang granite-syenite zone and its tectonic implication. Geol Rev 11:144–151 **(in Chinese with English abstract)**

Zhou JB, Zheng YF, Zhao ZF (2003) Zircon U–Pb dating on Mesozoic granitoids at Wulian, Shandong province. Geol J China Univ 8:185–194 **(in Chinese with English abstract)**

Zhou HS, Ma CQ, Chen L (2009) Petrogenesis and tectonic implication of Yanzigang alkali pluton in the Dabie orogenic belt: constraints from the zircon U–Pb ages and geochemistry. Acta Petrol Sin 25:109–1091 **(in Chinese with English abstract)**

Zou HB, Zindler A, Xu XS, Qi Q (2000) Major, trace element, and Nd, Sr and Pb isotope studies of Cenozoic basalts in SE China: mantle sources, regional variations and tectonic significance. Chem Geol 171:33–47